86-3459

How Accurate is Mathematical Fire Modeling?

Henri E. Mitler
John A. Rockett

U.S. DEPARTMENT OF COMMERCE
National Bureau of Standards
National Engineering Laboratory
Center for Fire Research
Gaithersburg, MD 20899

December 1986

U.S. DEPARTMENT OF COMMERCE
NATIONAL BUREAU OF STANDARDS

NBSIR 86-3459

HOW ACCURATE IS MATHEMATICAL FIRE MODELING?

Henri E. Mitler
John A. Rockett

U.S. DEPARTMENT OF COMMERCE
National Bureau of Standards
National Engineering Laboratory
Center for Fire Research
Gaithersburg, MD 20899

December 1986

U.S. DEPARTMENT OF COMMERCE, Malcolm Baldrige, *Secretary*
NATIONAL BUREAU OF STANDARDS, Ernest Ambler, *Director*

TABLE OF CONTENTS

LIST OF FIGURES

HOW ACCURATE IS MATHEMATICAL FIRE MODELING?

Henri E. Mitler and John A. Rockett

Abstract

It is important to be able to predict the development of a fire in an enclosure of arbitrary complexity. A mathematical model valid for a single room, with multiple vents and objects in it has been developed. The fifth version of the model has just been completed*; it is the Harvard Computer Fire Code V, or Mark 5 for short. In 1977, Factory Mutual Research Corporation carried out a series of eight well-instrumented full scale room fires, against which the single room model can be tested. The test fire room was 2.4 m x 9.6 m x 2.4 m high, with an open doorway; a slab of polyurethane foam in one corner, and a polyurethane foam target in a facing corner. The primary slab was ignited at its center, and the fire followed. The other tests were variants of this one. We compare the results of the calculations with the results of two of the experiments: the standard configuration and the case with a window replacing the doorway. The model "predictions" are in good to excellent agreement for most of the variables. The disagreements are discussed, and it is found that the most probable causes are: failure to take heating of the bottom gas layer into account, inadequacy of the burnout algorithm, and the lack of understanding of the CO-production mechanism.

*This article is based on a paper presented at the US-USSR Scientific Exchange Meeting, Tbilisi, USSR, July 1981, which has appeared in Russian. The long delay in publication is partly due to an agreement with the USSR to wait for preliminary Russian publication. There has since then been substantial development of Mark 5 (see ref. [21]).

Keywords: CFC V; compartment fires; computer modeling; Mark 5; Mark V; room fires.

1. INTRODUCTION

The growth of a fire in a building is an extremely complex phenomenon. Nevertheless, with modern scientific tools, it should be amenable to analytic prediction. Perhaps the first research in predicting fire behavior was that of Ingberg [1] at the National Bureau of Standards. He considered the effect of amount of fuel (fuel loading) on fully-involved room fires; Kawagoe [2] improved the analysis by taking ventilation into account. The last decade has seen a rapid development in the understanding of fire physics and in synthesizing and quantifying this understanding in analytic models. These advances will not be reviewed here. Good bibliographies can be found in Mitler [3] and Babrauskas and Williamson [4]. Much has also been learned about physically modeling fire (Heskestad [5]). However, this discussion will be confined to mathematical modeling.

A significant feature of recent fire models is their attention to the initial growth of fire from a small ignition source to full room involvement (flashover), and beyond. This is in response to the belief of many fire protection engineers that fire can be controlled before flashover. Emphasis on the early fire has been possible because the physics of fire is now much better understood than it was only ten or fifteen years ago.

The pre-flashover fire is inherently more complicated than the post-flashover fire, but the development of modern computers permits the solution of the equations, at least in some restricted form.

There are basically two kinds of mathematical models. First, "field" (or continuum) models, where the Navier-Stokes equations are used for the fluid flows, together with equations describing the combustion and radiation. Second, "zone" models, which employ much-simplified equations to describe each of the several phenomena which can be conceptually isolated in a zone. The latter seem (for the moment) more practical, since the solutions of their equations, even in the time-dependent case, are literally orders of magnitude faster than the solution of the more nearly exact field equations. Zone models are able to represent a much more varied physical content than field models but at the cost of much less spatial resolution. There is a degree of artistry (or arbitrariness) involved in zone "modeling", since the models representing each phenomenon must be simultaneously reasonably accurate yet simple enough to be described by equations which are readily solved.

Numerous studies have been carried out with zone models; of particular note is the work of Quintiere [6], MacArthur [7], Pape [8], and Emmons, Mitler, and Trefethen [9]. A survey of recent developments in modeling is given by Friedman [10].*

Ultimately, it should be possible to predict the development of a fire in an enclosure of arbitrary complexity. What has been achieved so far is a fair simulation of what happens in a single room with multiple vents and one or more objects. Several multi-room models are also available of which the most elaborate is probably that of Tanaka [11]. His model, however, while allowing for multiple rooms at multiple levels, assumes a fire with a prescribed energy release rate as a function of time. There are strong similarities among the

*Also see refs. [22] and [23].

single room zone models currently in use although they differ in detail. In this paper attention is focused on the simulation developed at Harvard over the past seven years. The latest major revision of this computer program is called the Harvard Fire Code V, or Mark 5 for short. It simulates fire in a single room vented directly to ambient air. It allows for up to five vents and five combustible objects. Each object can heat up and possibly ignite. The simulation allows for one of three possible initial fires: a burner fire--i.e., one of constant radius and heat release rate, a pool fire--i.e., one of constant radius, and a growing fire--one ignited over a small area, which then spreads.

This paper will describe the principal features of the Harvard Mark 5 simulation and then compare its predictions for two fires with the experimentally observed behavior.

2. SCOPE OF THE MODEL

We will describe some of the pheonomena which take place when a fire is ignited in a room, below. This has been done in more detail elsewhere (see, for example, ref. [3]). Most of the important physical effects involved in a room fire have been explicitly taken into account in Mark 5, to one or another degree of approximation [3,9-13]. The phenomena not included are mainly associated with post-flashover behavior or events immediately preceding flashover. Although classed as a zone model, the zones of Mark 5 are not necessarily clearly delineated subdivisions of the room volume. They are: (1) the objects, (2) the fire plumes over any objects which are burning,

(3) the layer of heated gas trapped under the ceiling (assumed to have a sharply delineated lower surface although, in practice, this may not be the case), (4) the ceiling and that portion of the walls in contact with hot gas layer, (5) the floor and lower walls, (6) the vents. Note that the vents are a phenomenological zone but physically a boundary between the inside and outside of the room. Some of the phenomena associated with the zones are: (a) entrainment of air into the hot, buoyant plume produced by the fire, (b) the production of soot and gaseous combustion products and depletion of oxygen in the plumes, (c) the (transient) formation of the hot layer under the ceiling, (d) radiative energy exchange between the fire plume, hot layer, upper and lower walls, ceiling and floor and with the space outside the vents, (e) the heating of the ceiling and upper walls and the objects in the room, (f) ignition of objects not initially burning, either through auto-ignition or by flame contact, (g) mass flow through the vents. Some situations not currently included are: (1) vents located in the ceiling, (2) external winds, (3) mixing at the vents between the hot exiting fire gases and entering ambient air, together with effects associated with this mixing on the lower, cool gas layer, (4) the effect of pre-ignition pyrolysis, burning in vitiated air and upper layer flashover, (5) the effect of sprinklers or other extinguishers. Although CO production is calculated, the present method for doing this reflects our very imperfect understanding of the production mechanism and is based on very limited data correlations. Finally, the effects of initial stable gas stratification, gas compression and finite transit times have been assumed to be of minor importance. This last could become a problem were Mark 5 used for estimating the performance of fire detectors in high ceilinged rooms.

In the following paragraphs, a brief outline of the equations defining the model will be given. This has already been done in some detail by Emmons [12], and in more detail in reference [9]. The model has, of course, evolved since these reports were written, and the more comprehensive set of equations is found in references [3] and [13].

Figure 1 shows the situation to be simulated a few mintues into the fire, and some of the room dimensions (h) and selected variables, such as the mass flows ($\dot{m}$) and radiative fluxes (ϕ).

3. MODELS OF THE PHYSICAL PROCESSES

3.1 The Burning Object

As stated above, Mark 5 allows for three types of fires: a gas burner, a pool fire or a growing fire. The growing fire algorithm is the most general, the other two are specializations of this. The growing fire model is for a centrally ignited horizontal slab of material. It was experimentally observed that, for foamed polyurethane, the fire radius increases exponentially with time [14]. We assume that the spread rate depends on the net impinging flux in such a way that the experimentally-observed exponential growth rate for a small fire is reproduced. Reradiation and convective heating of the burning surface are taken into account in calculating the net impinging heat flux. This leads to the spread-rate expression for the fire radius,

$$\dot{R} = AC\left(1 + \frac{C}{2} + \frac{C^2}{3}\right), \qquad R \leq 0.95\, R_m \tag{1}$$

where $C = \phi/\sigma T_f^4$ (2)

and A is a spread-rate parameter specific to the material. ϕ is the net heat flux impinging on the pyrolyzing surface, and T_f is the flame temperature. It will be seen that the right hand side of equation (1) represents the first three terms in the expansion of log(1-C). This was done in order to avoid the singularity at C = 1.

When the radius R approaches the input maximum radius, R_m, the spread rate evidently must go down, and so we take

$$\dot{R} = (R_m - R)/10, \qquad R > 0.95\ R_m \tag{3}$$

$\dot{R}$ is integrated to find the radius, R(t).

The pyrolysis rate is then given by

$$\dot{m}_f = - \pi R^2 \phi / H_v \tag{4}$$

where H_v is the heat of pyrolysis (or vaporization). The negative sign is included because $m_f(t)$ is the mass of the fuel.

An important point is that ϕ includes <u>all</u> the radiation incident on the surface, including that from the hot layer, walls, and its own flame and other fires. This feedback produces an acceleration of burning in the room, relative to burning in the open where only radiation from the objects own flame would be present.

Combustion in the diffusion flames found in fires is typically quite inefficient. Only a fraction of the pyrolyzed fuel in fact burns, the rest going off as soot, CO, and unburned hydrocarbons. Furthermore, when the hot upper gas layer is so low that it keeps the fire plume from entraining much air, the fire becomes starved for oxygen, and the burning rate may go lower still. Thus the burning rate is

$$\dot{m}_b = \min (- \chi \dot{m}_f, \dot{m}_e/\gamma) \qquad (5)$$

where $\dot{m}_e$ is the rate of entrainment of air into the plume, γ is the effective air/fuel mass ratio in burning, and χ is the fraction of pyrolyzed fuel which actually burns (completely). This is found from experiment to be about 14.45.* The chemical energy released then in either case is

$$\dot{Q} = \dot{m}_b H_c, \qquad (6)$$

where H_c = the heat of combustion

The burner and pool fires are rather simpler, and will not be described here.

3.2 The Flame

The flame is modeled by a homogeneous, isothermal gray cone of gas, of semi-apex angle, ψ. When the fire is starved for oxygen, or when near fuel exhaustion, the cone becomes squatter, thereby emitting less radiation. In

*Recalculation in 1985 showed that γ is closer to the stoichiometric value, 9.85.

the absence of other limiting factors the cone angle is $\psi_o = 30°$. When oxygen starvation or burnout reduce the burning rate, then

$$\tan \psi = \chi \tan \psi_o |\dot{m}_f| / \dot{m}_b \tag{8}$$

The flame gas temperature is taken to be 1260°K, and its absorption coefficient $k = 1.55\ m^{-1}$, in agreement with measurements made by Markstein [15] and Orloff [16]. Radiation per unit area to the flame base is then given by

$$\phi_b = \sigma T_f^4 \left(1 - e^{-4\xi kV/A}\right) \tag{7}$$

where V = cone volume, A = bounding area, and ξ = shape factor (or order 0.9). Radiation from the flame to other targets is complicated by the fact that the slab on which it "sits" may shade targets lying below it. Expressions for the flux to ceiling, targets (horizontal or vertical) and that absorbed by the hot layer, are given in references [3] and [13].

3.3 The Fire Plume

The plume model used is that due to Morton, Taylor and Turner [17] with the heat source a virtual point below the surface of the fuel at a distance such that the plume radius at the surface matches the fire radius:

$$x = R/1.2\alpha \tag{9}$$

Here, α = the entrainment coefficient, taken to be 0.1. The mass flow from the plume into the hot layer is

$$\dot{m}_p = \pi \rho_a \left(b^2 u - R^2 u_f\right) - \dot{m}_f$$

where ρ_a = ambient air density (1.177 kg/m^3 at 300°K)

$b = 1.2\ \alpha h'_p$ is the plume radius at the hot-cold layer interface

$h'_p = h_r - h_f - h_L + x$ is the height of the plume above the virtual source. Note that the plume height shown in figure 1 is $h_p = h'_p - x$.

h_r = room height

h_f = height of the fire base

h_L = depth of the hot gas layer

$u = \left(C_o/h'_p\right)^{1/3}$ is the axial flow velocity at the hot-cold layer interface

$u_f = \left(C_o/x\right)^{1/3}$ is the axial flow velocity at the fire base

$C_o = 25\ g\dot{Q}/48\ \pi\alpha^2 C_p T_a \rho_a$

T_a = ambient temperature

C_p = ambient air specific heat

g = acceleration of gravity

$\dot{Q}$ = rate of heat release in the plume

α = the entrainment coefficient = 0.1

Enthalpy is carried into the hot layer by the plume at the rate

$$\dot{E}_p = \dot{m}_p C_p T_a + \dot{Q} - \dot{E}_{pr} \qquad (16)$$

where $\dot{E}_{pr}$ is the energy lost by the plume *via* radiation (of the order of 35 percent of $\dot{Q}$).

3.4 The Hot Layer

In common with most zone models, two gas layers are assumed. The upper gas layer is homogeneous and isothermal, and the lower layer consists of ambient air. The interface between the two layers is assumed to be a horizontal plane. In reality, of course, there is seldom a distinct homogeneous "upper layer"--the temperature and species concentrations vary from point to point; a first simplification of reality would be to assume a single smoothly varying vertical *profile* for all locations within the room (except within the fire plumes). The step-function profile assumed for current two-layer models is a further simplification, but it seems adequate, so far.

An energy balance for the hot layer yields

$$\dot{E}_L = \sum_p \dot{E}_p - \sum_v \dot{E}_u - \dot{E}_c - \dot{E}_{LR} \qquad (17)$$

where $\dot{E}_p$ = the energy added from the fire plumes

$\sum_v \dot{E}_p$ = the energy carried out through the vents by mass flow

$\dot{E}_c$ = the energy convected into the walls

$\dot{E}_{LR}$ = the *net* loss of energy by radiation

Similarly, the layer mass changes according to

$$\dot{m}_L = \sum_p \dot{m}_p - \dot{m}_u \qquad (18)$$

where $\dot{m}_p$ = the mass added from the fire plumes

$\dot{m}_u$ = the rate at which mass leaves the room via the vent(s)

The layer mass and energy are then found by integrating equations [17] and [18].

Since we can also write

$$E_L = M_L C_L T_L = (\rho_L V_L) C_L T_L = \rho_L A h_L C_L T_L \qquad (19)$$

(where A is the cross-sectional area of the room, C_L is the specific heat of the hot layer gases, h_L is the layer depth, and ρ_L its (mass) density), we have

$$h_L = E_L / A C_L \rho_L T_L = E_L / A C_L \rho_a T_a \qquad (20)$$

where the second equality follows from the ideal gas law. If we ignore the (small) difference between C_L and C_p (the specific heat of ambient air, at constant pressure), it is clear that the layer depth is a function only of the layer energy. It also becomes clear that the total gas energy in the room is (essentially) constant: as energy is added, enough gas is pushed out by gas expansion, to leave the total energy unchanged. Finally, the layer temperature is found from

$$T_L = E_L / C_L M_L \qquad (21)$$

The oxygen concentration in the layer is readily found as the solution of the equation

$$\dot{m}_{ox} = 0.2318 \left[\dot{m}_L - \gamma_s \dot{m}_b\right] - Y_o \dot{m}_u \tag{22}$$

where $$Y_o = m_{ox}/m_L \tag{23}$$

is the mass fraction of oxygen in the hot layer and γ_s is the stoichiometric air/fuel mass ratio (9.85 for polyurethane); 0.2318 is, of course, the mass fraction of oxygen in air, and $\dot{m}_e$, $\dot{m}_u$, and $\dot{m}_b$ have all been defined already. As for the other chemical species, each burning material is assumed to generate a constant fraction of CO, CO_2, H_2O, soot, and hydrocarbons per unit mass of fuel pyrolyzed. Values for these fractions are taken from measurements [18] and the species concentrations in the hot layer thus become calculable. These concentrations, in turn, permit evaluation of the layer's absorptivity, k, which is then used in various radiation calculations. Two alternative routines are used to evaluate k. The simpler one assumes that <u>all</u> the absorption is due to (grey) soot absorption:

$$k = 265\ Y_s \tag{24}$$

where $$Y_s = m_s/m_L \tag{25}$$

is the soot mass fraction. The more complicated one also takes into account the band absorption of CO_2 and H_2O.

3.5 The Vents

The mass flows through each vent are calculated according to a hydraulic model [19], with an efflux coefficient of 0.68. The pressure at the floor in the center of the room is used as an auxiliary variable. As a result of assuming the gas layers to be, separately, homogeneous, the pressure difference across a vent is a piecewise linear function of height. The vent is divided into horizontal strips corresponding to each linear variation, and include any place where Δp drops to zero (a neutral axis) as a strip boundary. Then for the i^{th} strip, the pressure drop at the top of the strip:

$$\Delta p_{i+1} = \Delta p_i - \left(\frac{\rho - \rho_a}{\rho_a}\right) \Delta h_i \tag{26}$$

where Δp_i is the pressure drop at the bottom of the strip, ρ_a is the ambient air density, ρ that of the hot layer, and Δh_i the height of the strip. The mass flow through that strip then is

$$\dot{m}_i = G_i \frac{b + \sqrt{ab} + a}{\sqrt{b} + \sqrt{a}} \tag{27}$$

where $$a \equiv |\Delta p_i|, \; b \equiv |\Delta p_{i+1}| \tag{28}$$

and $$G_i = (\text{sign } \Delta p_i)\ (2/3)\ C_d B\ \Delta h_i\ \sqrt{2\ g \rho_a \rho} \tag{29}$$

Here $C_d = 0.68$ and B is the width of the vent. When Δp_{floor} is correctly chosen, all the flows are such that mass balance for the room is satisfied:

$$\dot{m}_R \equiv \dot{m}_{out} - \dot{m}_{in} = \frac{\dot{E}_L}{C_p T_a} - \dot{m}_L - \sum_f \dot{m}_f \tag{30}$$

3.6 Radiation

There are eight radiation subroutines which calculate the most important radiation exchanges among the flame(s), objects, hot layer, and hot wall/ceiling. Some are quite simple, like equation (7). Most others are complex, and will not be listed here; the interested reader should see reference [3].

3.7 Convective Heat Transfer

The convective heat exchanges between the hot layer and walls, and that between layer(s) and objects, are found assuming a simple (but temperature-dependent) film coefficient. For heat transfer to ambient air, Mark 5 takes

$$\dot{q}'' = h_e \left(T_s - T_a\right) \tag{31}$$

where $h_e = 5 \text{ w/m}^2\text{K}$

and T_s is the temperature of the surface being cooled (outside of walls, or objects in the room). For heat transfer <u>from</u> the hot layer,

$$\dot{q}_L'' = h_i \left(T_L - T_s\right) \tag{32}$$

where $$h_i = \min \left[50, 5 + 0.45 \left(T_L - T_a\right)\right] \tag{33}$$

In the steady state, the heat loss rate to the walls and ceiling therefore is

$$\dot{E}_{LW} = \dot{q}''_L A_W \tag{34}$$

where $$A_W = 2\ (L + W)\ h_L + LW - A_v \tag{35}$$

where L and W are the length and width of the room, and A_V is that part of the vent area intersected by the hot layer. Here T_s of equation (32) is taken to be T_W, the inner wall/ceiling temperature, assumed to be uniform. As the fire grows, however, the layer thickens and, in order to (artificially) maintain a uniform temperature, extra heat has to be supplied to the newly exposed wall areas. This must be done such that the newly heated wall immediately acquires the same temperature profile throughout its thickness as the rest of the heated wall. Hence for the <u>growing</u> layer, equation (34) is replaced by

$$\dot{E}_{LW} = \dot{q}''_L A_W + 2\ (L + W)\ q''\ \dot{h}_L \qquad (\dot{h}_L > 0) \tag{36}$$

where $$q'' = \int_0^t \left(\dot{q}''_L + \dot{q}''_{AW}\right) dt \tag{37}$$

is the energy per unit area stored in the wall, and $\dot{q}''_{AW}$ is given by equation (31), with $T_s \equiv T_{\text{outside wall surface}}$. It follows from equation (20) that

$$\dot{h}_L = h_L \dot{E}_L / E_L \tag{38}$$

When the layer <u>decreases</u> in depth, we evidently must use equation (34) rather than equation (36).

3.8 Conductive Heat Transfer

Walls and objects are assumed to be finite-thickness slabs insulated at their edges. Thus the one-dimensional heat-conduction equation can be used.

$$\frac{\partial T}{\partial T} = \alpha \frac{\partial^2 T}{\partial x^2} \tag{39}$$

is solved numerically with a simple algorithm. Although this finds the temperature profile through the object as a function of time, most of that information is neglected, as we are (currently) only interested in the surface temperatures and the integral of the profile.

This completes the brief outline of the physics included in the model.

The numerical methods by which the resulting equations are solved will not be discussed since this is done in detail in CFC III [9] and CFC V [13]. For those readers who are not familiar with these papers, we might mention that two alternative algorithms are used: a Gauss-Seidel successive substitution method is normally used; when convergence is not achieved with that method, a multivariate Newton technique is used. This combination works very well, 95 percent of the time.

4. THE TESTS

In 1977, Factory Mutual Research Corporation carried out [20] a series of eight well-instrumented full-scale room fire tests, against which the Mark 5 program can be checked. The eight tests were systematic variations of a

a standard room. The standard configuration is shown in figure 2; it is a 2.44 by 3.66 by 2.44 m room (8' x 12' x 8') with an open doorway 0.76 x 2.03 m (30" wide by 80" high); a slab of polyurethane (P.U.) foam, measuring 1.52 x 1.52 x 0.10 m (5' x 5' x 4") is in one corner; its top surface is 61 cm from the floor (this models a foam mattress). A P.U. foam target 1.22 x 0.30 x 0.10 m (4' x 1' x 4") is in the near adjacent corner; its top surface is 25 cm (10") above that of the primary fuel slab. The primary slab is ignited at its center, and the fire followed.

Tests #0, 1, and 2 were all meant to be identical--the standard configuration. Test 3 had the doorway narrowed to 19 cm; test 4 added a window; test 5 had a pool of PMMA beads replacing the foam; test 6 had a window instead of a door, and test 7 had the door reaching up to the ceiling. Comparing the results of calculations with the results of these experiments shows that the "predictions" vary from excellent to fair for most of the variables. Although comparisons have been made for all the tests, for brevity only two of these will be discussed: the standard configuration and test #6. These show the best and poorest agreements between the predictions of the model and the actual fires.

5. RESULTS

The rate of mass loss of the fuel (while it is burning) is shown for runs 0, 1, and 2, in figure 3. These are curves A, B, and C, respectively. We see that A and B agree very well, although there is a good deal of statistical fluctuation for $t < 150$ sec. For test #2 (on July 8) fire development was more rapid, as can be seen from curve C--it looks as if ignition occurred

about 40 seconds early. Note that these are semilog plots, as is also true for figs. 6, 11, 12, and 13.

The thickness (or depth) of the hot gas layer for each of these first three tests is shown in figure 4. Up to t = 200 sec, curves A and C (tests 0 and 2) track together very well, whereas curve B (the dotted curve, corresponding to test 1) begins its descent some 50 sec earlier; this contrasts with the behavior in fig. 3, where ignition appeared to have occurred earlier for test 2, rather than test 1. Beyond 200 sec, B and C switch - that is, curve C leads the other two by about 40 sec (consistent with the mass-loss rate shown in fig. 3), while A and B track together quite well. This holds up to t = 310 sec; after that, there are substantial deviations, curve B displaying marked oscillations whose nature is not clear. These two figures serve to show how much variation there can be in reasonably well-controlled experiments--so that we should not expect calculated results to agree any better than this, with any one experimental fire.

Test #1 (July 6) was used as the standard for comparison, partly because a roof leak appeared during test #0, and it is, therefore, suspect. The target ignited 310 seconds after ignition of the primary slab, and the sprinkler was turned on at t = 326 sec.

Figure 5 shows how differences in the handling of the <u>data</u> can also lead to rather different results. The solid curve shows "the temperature" $T_L(t)$ of the hot layer as a function of time, as obtained by taking an average of the readings of 8 thermocouples located at different places in the room, all at a height 1.71 m from the floor--(70 percent of the distance to the ceiling).

This was the value of $T_L(t)$ used by Factory Mutual in their data analysis. We made a different evaluation of $T_L(t)$, using the temperature profiles as a function of height at three places in the room; this gave the dashed curve. As can be seen, the latter method gives a peak temperature 150°C lower than the FMRC method does.

6. PREDICTION VS EXPERIMENT

Figure 6 shows the pyrolysis rate for test #1 (July 6). The calculation generally agrees with experiment, though the maximum is some 50 percent high. Figure 7 shows the hot layer temperature for the same test. As we see, the calculation agrees quite well with experiment, out to 310 sec., but then falls below the experimental value. Incidentally, no meaningful comparisons can be made after t = 326, when the sprinkler was turned on--the program does not yet simulate extinguishment. Note that the calculated peak temperature is low even though the burning rate is over-predicted at this point.

In figure 8 the layer height calculation is shown to agree very well with experiment out to t = 290; the subsequent disagreement occurs in part because in Mark 5, the layer cannot descend below the level of the base of the fire. It is possible, moreover, that late in the fire the interface between the hot and cold layers is not, in fact, a plane: it may be that the surface rises locally, near the fire, and is lower elsewhere; because of the way in which it was obtained the data would only reflect the lower part of the surface.

The outflow rate of hot gas is shown in figure 9--again, the calculation is in excellent agreement with experiment out to t = 300 sec.; beyond that,

the hotter layer produces greater buoyancy (recall figure 7), and therefore greater flow. The target temperature (not shown) also agrees very well with calculation.

Figure 10 shows that the oxygen concentration in the layer is reasonably well calculated. The fact that the real minimum is lower than the calculated minimum is of course consistent with the temperature and mass flow curves, though a possible alternative explanation will be given when we discuss test #6.

Other species concentrations are shown in figure 11; the calculated CO_2 concentration agrees very well with experiment, but the CO does not.

The radius of the fire as a function of time is well predicted by the program, as is the radiative flux at the center of the floor (most of the radiation comes from the hot layer); see figure 12. (The calculated flux rises too slowly beyond t = 305 because the calculated layer temperature rises too slowly there.)

In sum, the standard run reproduces the results of tests 0 and 1 quite well, the principal disagreement being the failure to reproduce the temperature peak, and the consequences which flow therefrom.

Next, consider test #6, where the doorway was replaced by a window about 1 m high. $\dot{m}_f$, T_L, h_L, $\dot{m}_u$, T_w and $y(O_2)$ will be used for comparison.

The pyrolyzation rate, $\dot{m}_f$, (see fig. 13) is in excellent agreement up to t = 300, but the calculated peak again continues to rise beyond the experimental peak. In spite of that, the calculated temperature, T_L, rises more slowly than the experimental value, as seen in figure 14, and dies out much faster, beyond t = 360.

The layer depth in the room, h_L, is shown in figure 15, and is seen to agree reasonably well with experiment between t = 90 and t = 230. Beyond that point, the layer is again quite a bit deeper than calculated. The disagreement is bad after t = 360, just as it is for the temperature; however, the experimental values are themselves suspect out here.

The resulting gas outflow rate, $\dot{m}_u$, is shown in figure 16, and is in surprisingly good agreement with experiment out to $t \tilde{=} 210$. The first calculated maximum, at 280 seconds, is due to oxygen starvation: the layer is so low that not enough fresh air is drawn in by the plume to permit burning as in the open. The second maximum (at t = 350) is due to the beginning of burnout of the primary fuel. The third peak, at t = 380, is not understood.

In figure 17, we show the average temperature of the ceiling and upper part of the walls (that part in contact with the hot layer) T_w. As could be expected, the curves are similar to the layer temperature curves (see fig. 14)--that is, the calculated wall temperature lags behind the measured temperature by about 15 sec, out to t = 290, then falls behind more dramatically.

The oxygen concentration at the window, $y(O_2)$, is shown in figure 18 as a function of time for probes at different heights. Note that in this figure

The heights refer to distance down from the ceiling. Thus the curve marked 0.2H gives the oxygen concentration 20 cm below the ceiling. The stratification of the layer, which was not evident in test #1, is brought out most strikingly, here. It is clear from examination of the test data that there may well have been variations along the length of the room. (The stratification, incidentally, has important implications for burning in the vitiated layer.) Were the layer to be well stirred, the mean oxygen concentration would evidently be a weighted average of the experimental values. This average was not taken, but it is probable that the calculated O_2 concentration would agree reasonably well with such a mean.

Finally, the fact that the oxygen concentration at the fire base is ambient throughout most of the burn in spite of the fact that the layer has fallen below the base of the fire, is not consistent with the assumption that the layer is flat everywhere. It is much more likely that it rises locally, near the fire, as mentioned earlier.

7. DISCUSSION

The Mark 5 growing fire algorithm predicts the radius of the fires quite well. The same is true of the pyrolysis rates early in the fire; however, the predicted peaks tend to be too high, and the resulting burnout too swift.

The vent routine is quite good, and gives mass flow rates in excellent agreement with measurement provided the layer temperature is well predicted.

The plume model we use, though crude, seems satisfactory, judging only by the amount of air entrained and the resulting oxygen and CO_2 concentrations in the layer. The flux from the hot layer to the floor agrees well with experiment, suggesting that the layer emissivity is reasonably well estimated, and therefore that the smoke concentration is reasonably well predicted.

On the other hand, the wall temperatures are a bit low, suggesting that radiation from the flame plus convection from the layer are under-estimated. This suggests that the flame model is not quite adequate. This impression is reinforced when we note that the flux to the targets is low in some cases (but not in others).

The burnout of the fuel was made ad hoc, and turns out to be poor. This is not of central significance at the moment, but clearly has to be improved.

Because CO is a major hazard of fire the failure of the model to predict its concentration well is a major weakness. CO production in diffusion flames is not well understood and the model reflects this. Fortunately, research currently in progress shows promise that a better understanding of the physics and chemistry of CO production will soon be available.

Perhaps the most puzzling question is why the layer temperature is well predicted for most of the burn, but underpredicted late in the fire. There are at least five possible reasons for this:

1. Mark 5 may overestimate the rate of heat loss by the layer.

2. There may be burning in the layer itself.

3. The plume model may be inadequate, calculating more ambient air entrainment than is found in practice.

4. Mark 5 neglects heating of the lower layer; this may be important.

5. Air may be drawn up around the base of the flames. Mark 5 may limit burning due to oxygen starvation prematurely.

Let us consider these in order: #1 is very unlikely since it would lead to wall temperatures higher than observed, rather than lower. Also, energy loss through the vent is already underestimated. #2 is unlikely, as no thermocouple gave a reading anywhere near flame temperature. (However, the thermocouple response times may be too long.) #3 is possible, though not very likely. Heating of the lower layer, however, (#4) certainly occurs--both because the floor is heated by radiation, thereby heating the air, and by entrainment of the hot gases by the ambient air coming in through the vents. This will make the upper layer hotter, too.

The other effect which has been neglected, is the raising of the hot/cold interface at the fire. This would delay oxygen starvation, and allow more vigorous burning to take place. These are matters to be investigated, both theoretically and experimentally.

8. CONCLUSIONS

The overall performance of the Mark 5 simulations is satisfactory, both in its numerical stability and convergence, and in the predictions it makes. There are a small number of inadequacies, which are being investigated; there is every reason to believe these difficulties will be overcome.

In spite of all their complexities, therefore, it appears that fires can be successfully simulated by mathematical models, and it is clear that continued efforts will lead to continued progress.

9. REFERENCES

[1] Ingberg, S.H., Q. NFPA 20, 243 (1927). ibid 43 (1928).

[2] Kawagoe, K., Fire Behavior in Rooms (BRI Report No. 27), Building Research Institute, Tokyo, 1958.

[3] Mitler, H.E., The Physical Basis for the Harvard Computer Fire Code, Harvard University Home Fire Project T.R. #34 (1978).

[4] Babrauskas, V. and Williamson, R.B., Fire and Materials, Vol. 2, No. 2, 39 (1978).

[5] Heskestad, G., Modeling of Enclosure Fires, in Fourteenth International Symposium on Combustion, p. 1021 (1973).

[6] Quintiere, J., The Growth of Fire in Building Compartments, paper delivered at ASTM-NBS Symposium on Fire Standards and Safety, at NBS, Gaithersburg, MD (1976).

[7] Reeves, J.B. and MacArthur, C.D., 3-volume report, FAA-RD-120, Univ. of Dayton Res. Inst., Ohio (1976).

[8] Pape, R. and Waterman, T., RFIRES, Illinois Inst. of Tech. Res. Inst., Report J6367 (1976).

[9] Emmons, H.W., Mitler, H.E., and Trefethan, L. (Jr.), Computer Fire Code III, Harvard Home Fire Project T.R. #25 (1978).

[10] Friedman, R., Status of Mathematical Modeling of Fires, Factory Mutual Research Corp. Technical Report RC81-BT-5 (1981).

[11] Tanaka, T., A Model on Fire Spread in Small Scale Buildings, Third U.S.-Japan Panel on Fire Research and Safety, Building Res. Inst., Tokyo (1978).

[12] Emmons, H.W., The Prediction of Fires in Buildings, 17th International Symposium on Combustion (1979), p. 1101.

[13] Mitler, H.E. and Emmons, H.W., The Fifth Harvard Computer Fire Code, Harvard Home Fire Project T.R. #45 (1980).

[14] Orloff, L., Preliminary Testing of Polyurethane Slab, Factory Mutual Research Corp. Technical Report, May 23, 1977.

[15] Markstein, G.H., Scanning Radiometer Measurements of the Radiance Distribution in PMMA Pool Fires, 18th International Symposium on Combustion (1980), The Combustion Institute, p. 537.

[16] Orloff, L., Simplified Radiation Modeling of Pool Fires, 18th International Symposium on Combustion (1980), p. 549.

[17] Morton, B.R., Taylor, G.I., and Turner, J.S., Turbulent Gravitational Convection from Maintained and Instantaneous Sources, Proc. of Royal Society (London), Vol. A234, 1 (1956).

[18] Tewarson, A., Heat Release Rates from Burning Plastics, J. Fire and Flammability, Vol. 8, 111 (1977); and in several technical reports for Factory Mutual Research Corp.

[19] Prahl, J. and Emmons, H.W., Fire-Induced Flow Through an Opening, Combustion and Flame, Vol. 25, 369 (1975).

[20] Alpert, R.L., et al., Influence of Enclosures on Fire Growth, Vol. I: Test Data (Tests 0-7), Factory Mutual Research Corp., Serial No. 0A0 R2.BU0-7 (1977).

[21] Mitler, H.E. and Rockett, J.A., User's Guide to FIRST, A Comprehensive Single-Room Fire Model, National Bureau of Standards Internal Report, NBSIR to be published.

[22] Parikh, J.S., et al., Survey of the State of the Art of Mathematical Fire Modeling, Underwriters Laboratories Report, File NC554 (1983).

[23] Mitler, H.E., Comparison of Several Compartment Fire Models: An Interim Report, NBSIR 85-3233 (1985).

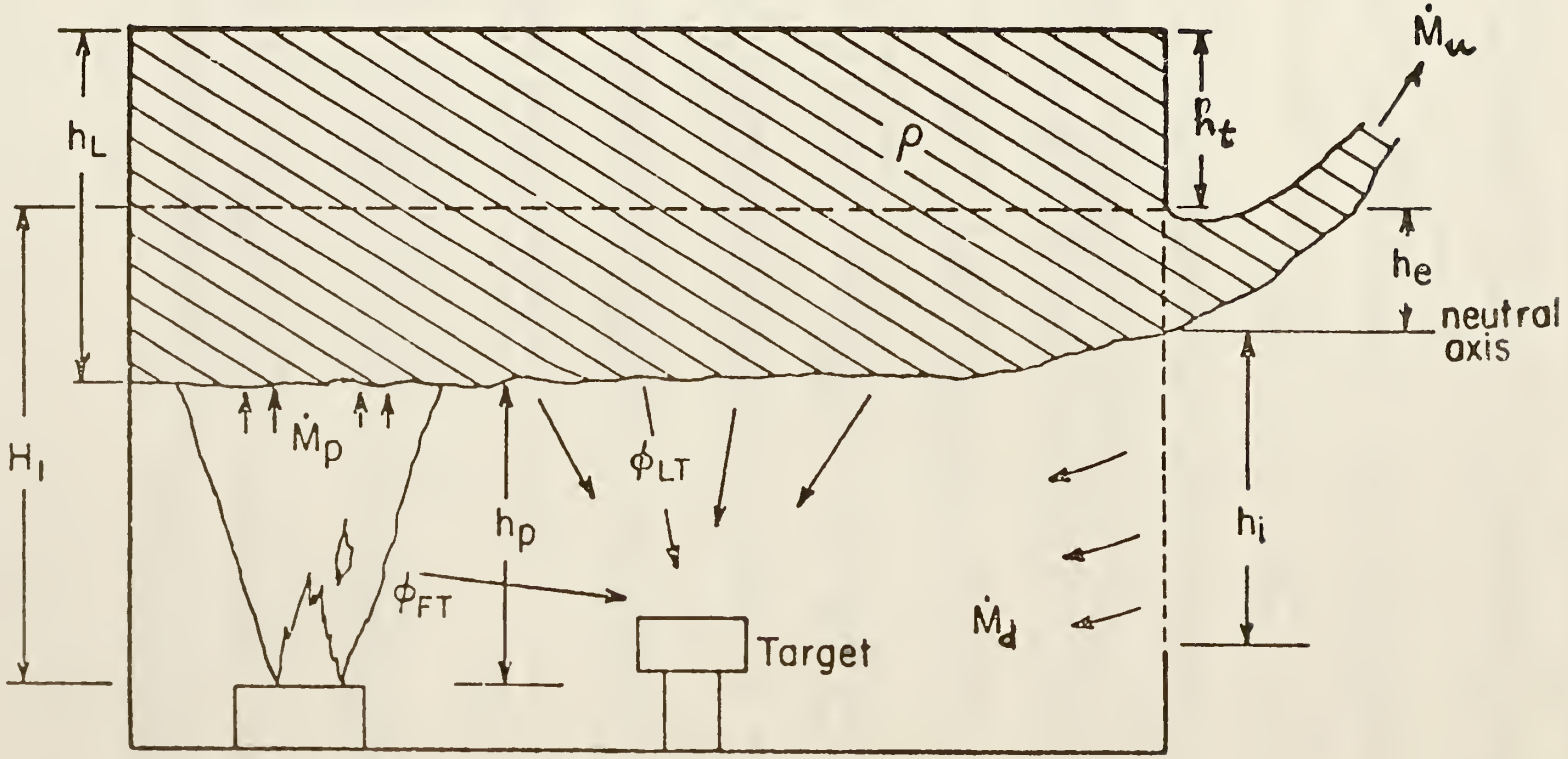
$\dot{M}_u$
h_L
ρ
h_t
h_e
neutral axis
H_l
$\dot{M}_p$
ϕ_{LT}
h_p
h_i
ϕ_{FT}
Target
$\dot{M}_d$

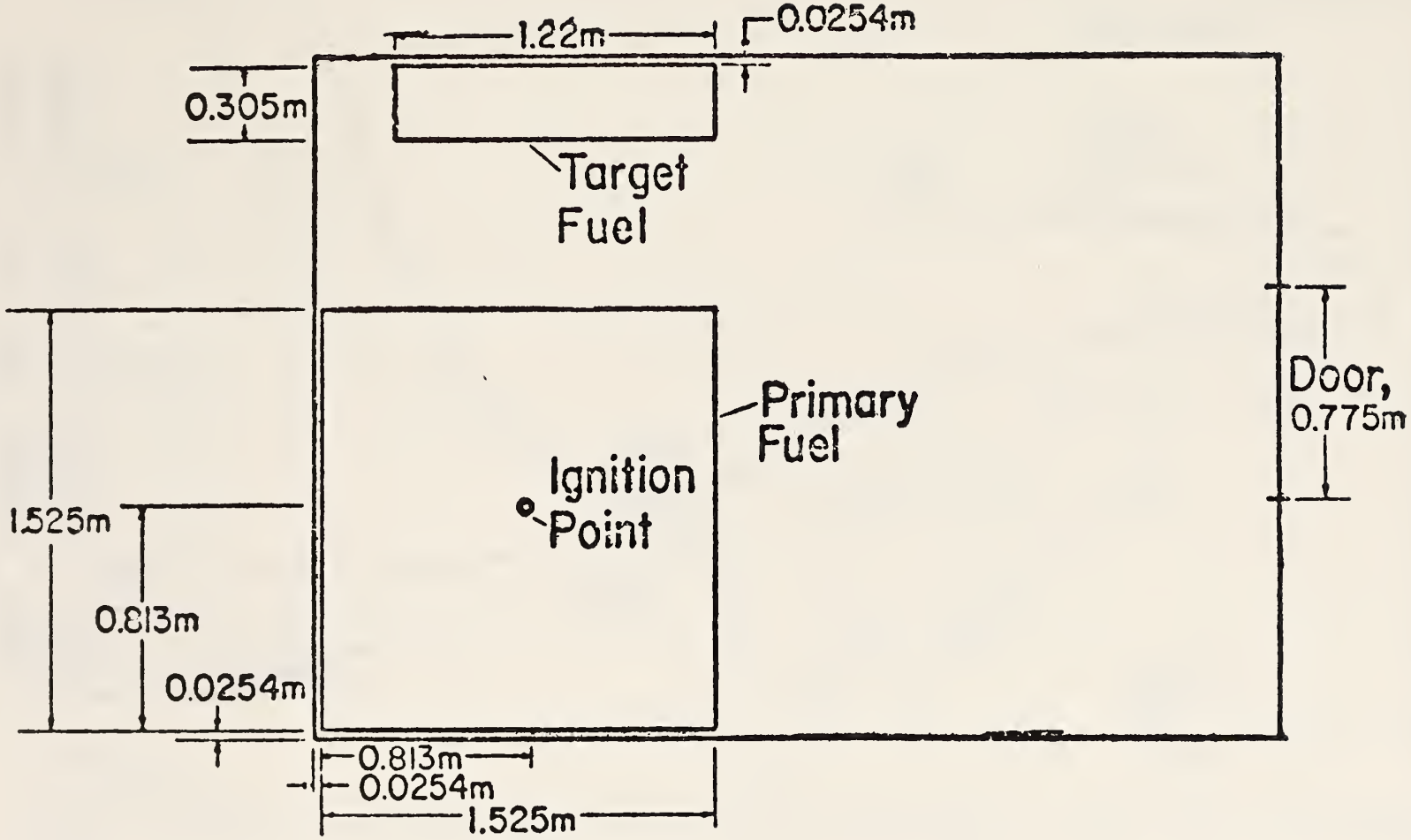
1.22m
0.0254m
0.305m
Target
Fuel
Primary
Fuel
Ignition
Point
Door,
0.775m
1.525m
0.813m
0.0254m
0.813m
0.0254m
1.525m

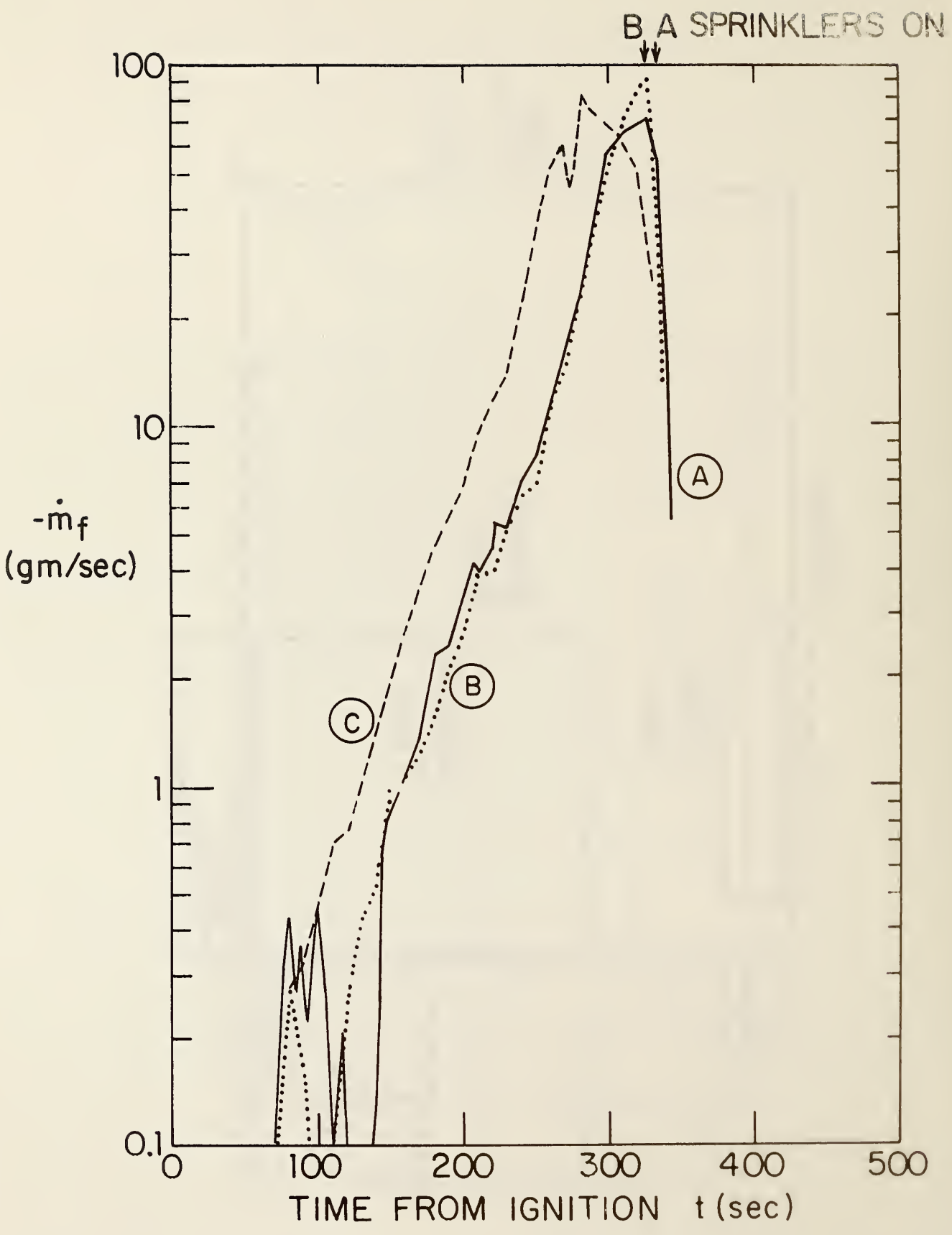
B A SPRINKLERS ON
100
10
1
0.1
$-\dot{m}_f$
(gm/sec)
A
B
C
0
100
200
300
400
500
TIME FROM IGNITION t (sec)

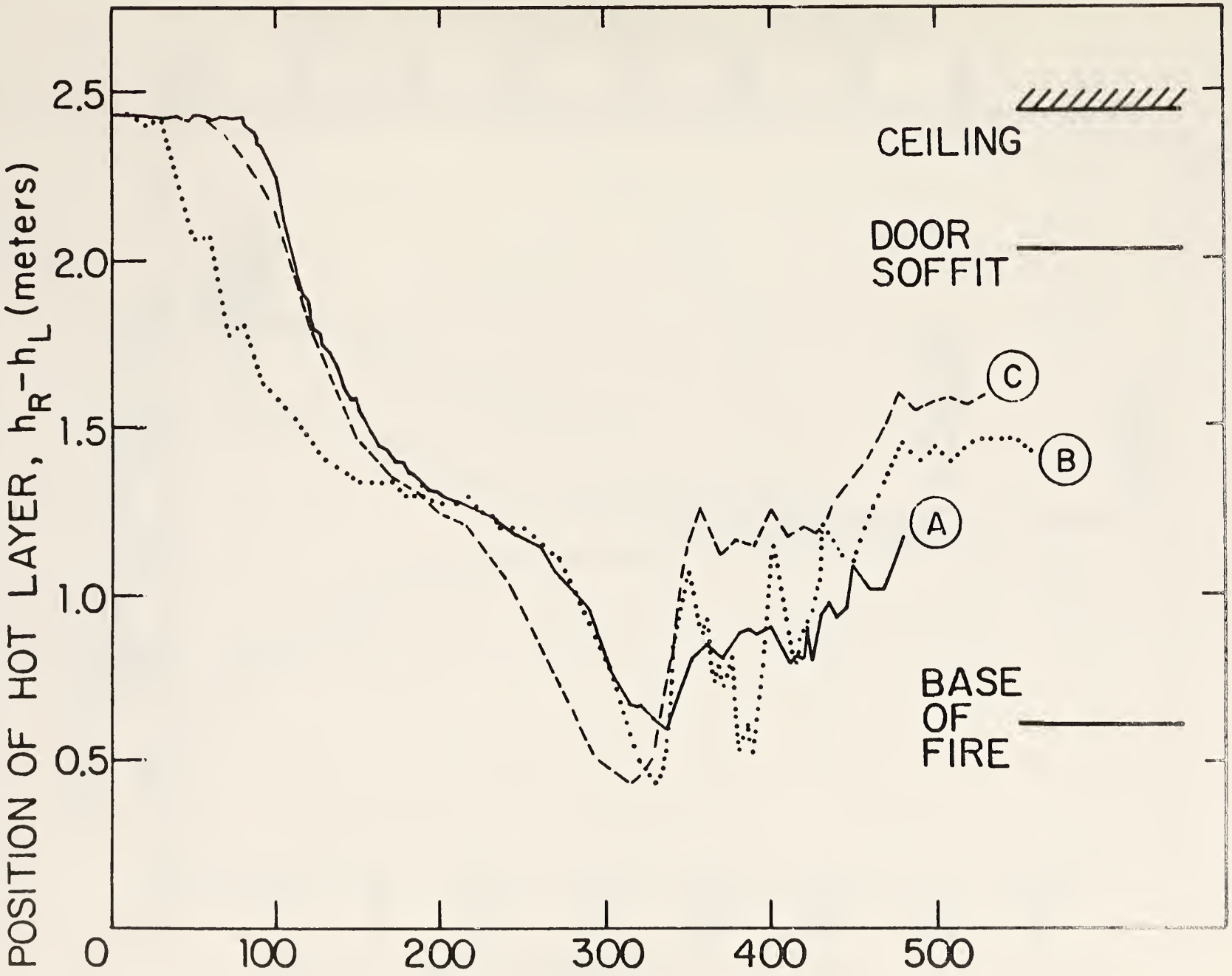
POSITION OF HOT LAYER, $h_R - h_L$ (meters)
2.5
2.0
1.5
1.0
0.5
0
100
200
300
400
500
CEILING
DOOR SOFFIT
BASE OF FIRE
A
B
C

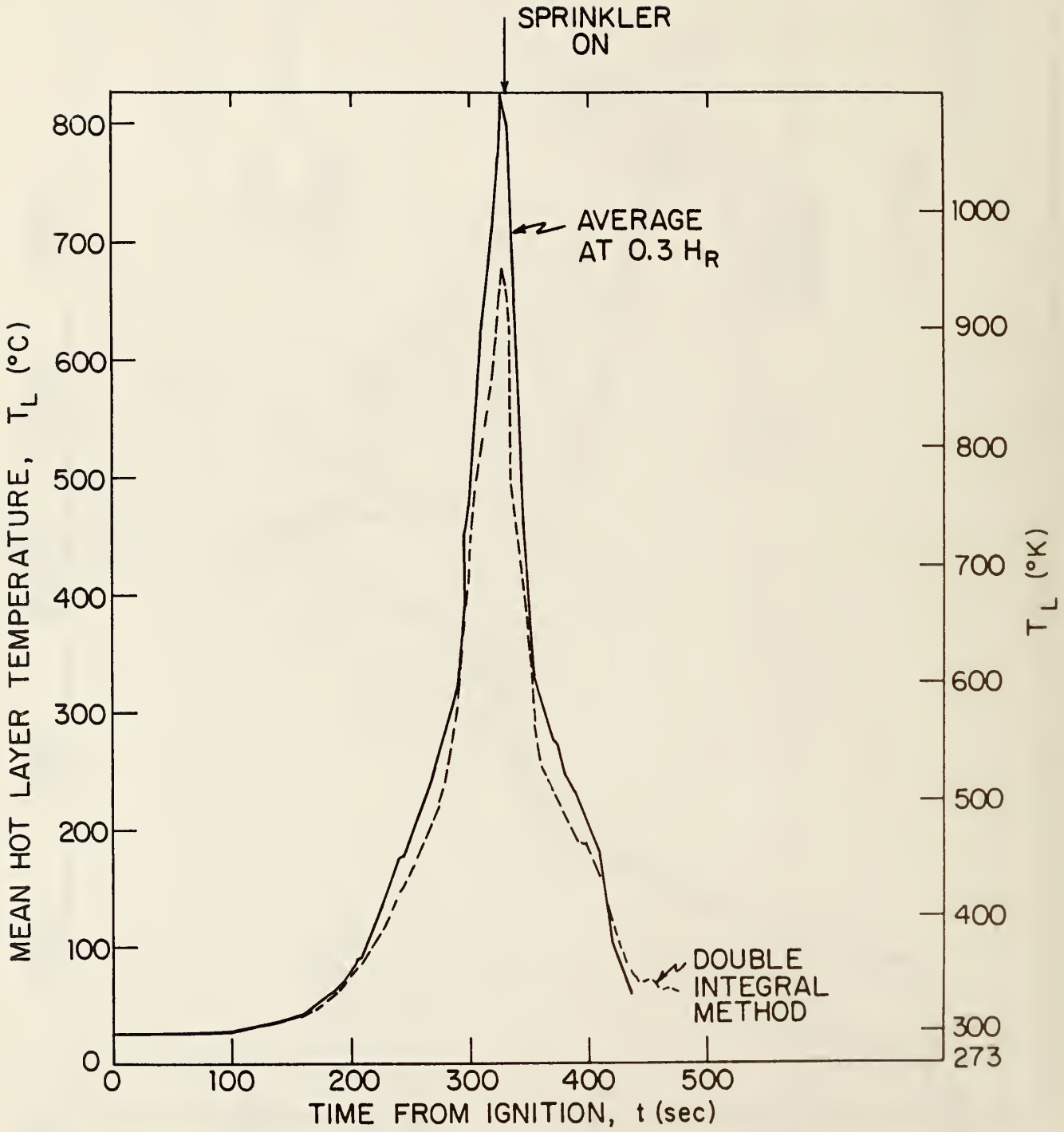
SPRINKLER
ON
AVERAGE
AT 0.3 H_R
DOUBLE
INTEGRAL
METHOD
MEAN HOT LAYER TEMPERATURE, T_L (°C)
T_L (°K)
TIME FROM IGNITION, t (sec)
0
100
200
300
400
500
600
700
800
900
1000
273

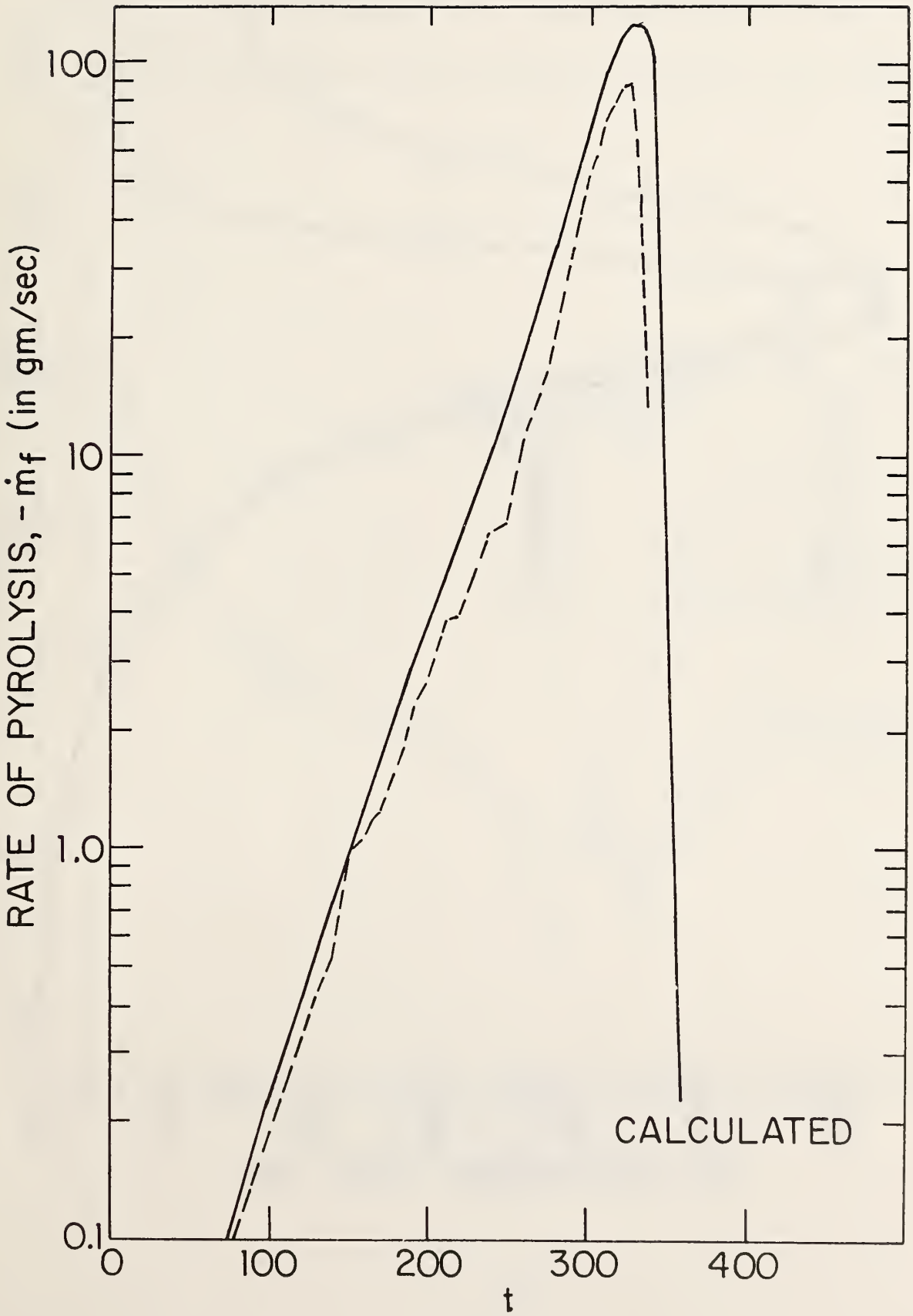
100
10
1.0
0.1
RATE OF PYROLYSIS, - $\dot{m}_f$ (in gm/sec)
0
100
200
300
400
t
CALCULATED

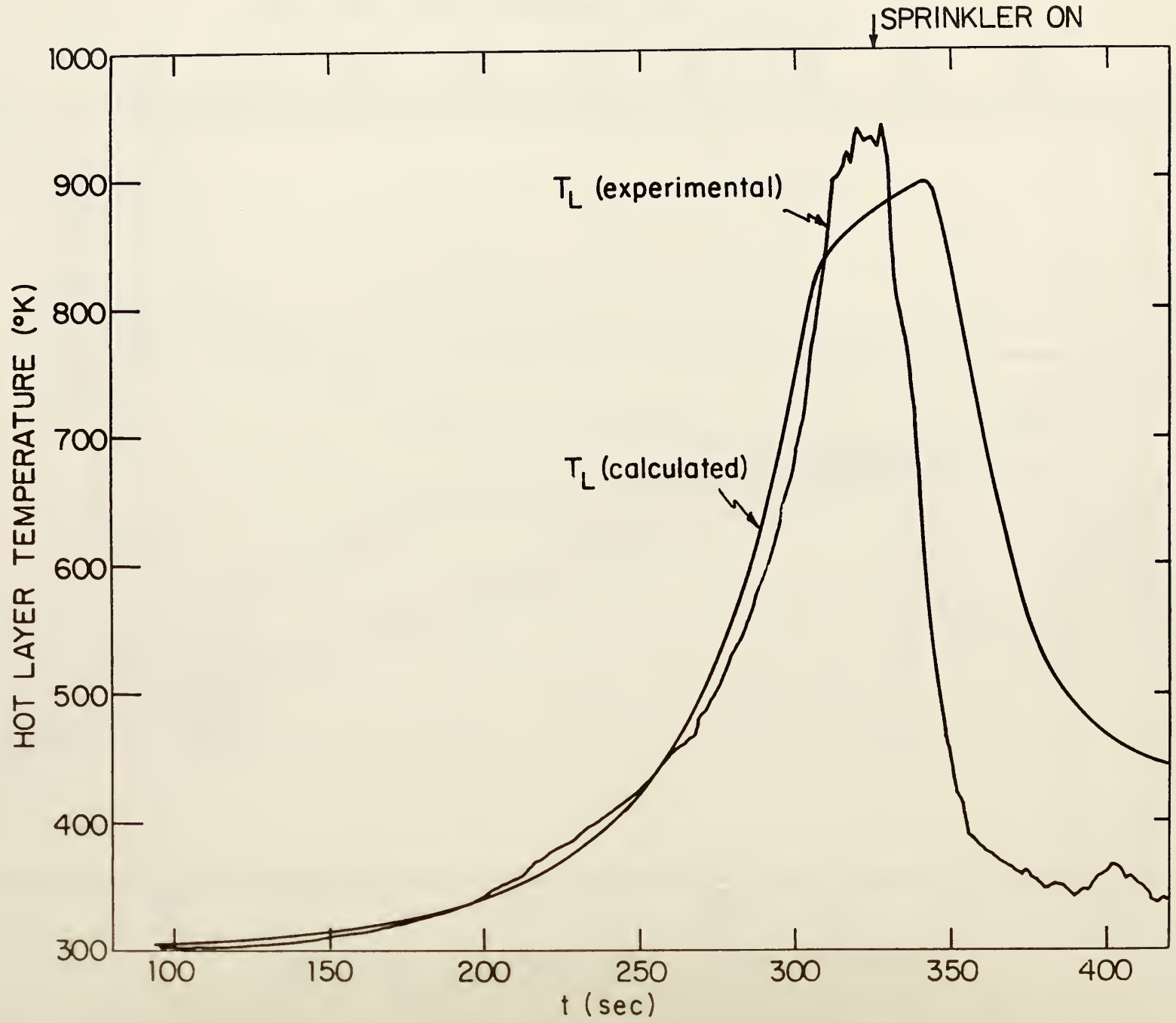
SPRINKLER ON
1000
900
800
700
600
500
400
300
HOT LAYER TEMPERATURE (°K)
T_L (experimental)
T_L (calculated)
100
150
200
250
300
350
400
t (sec)

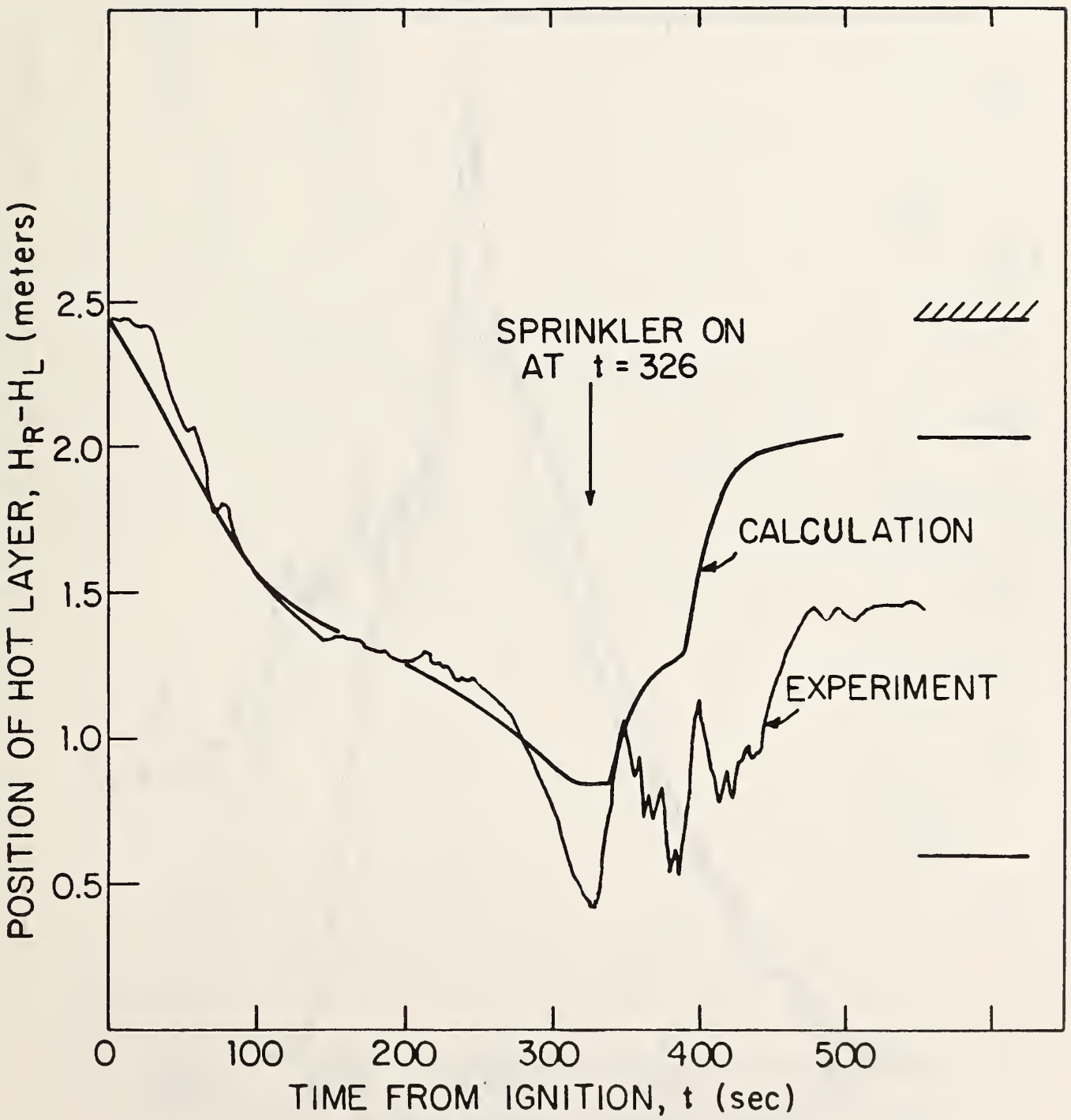
SPRINKLER ON
AT t = 326
CALCULATION
EXPERIMENT
POSITION OF HOT LAYER, H_R-H_L (meters)
2.5
2.0
1.5
1.0
0.5
0
100
200
300
400
500
TIME FROM IGNITION, t (sec)

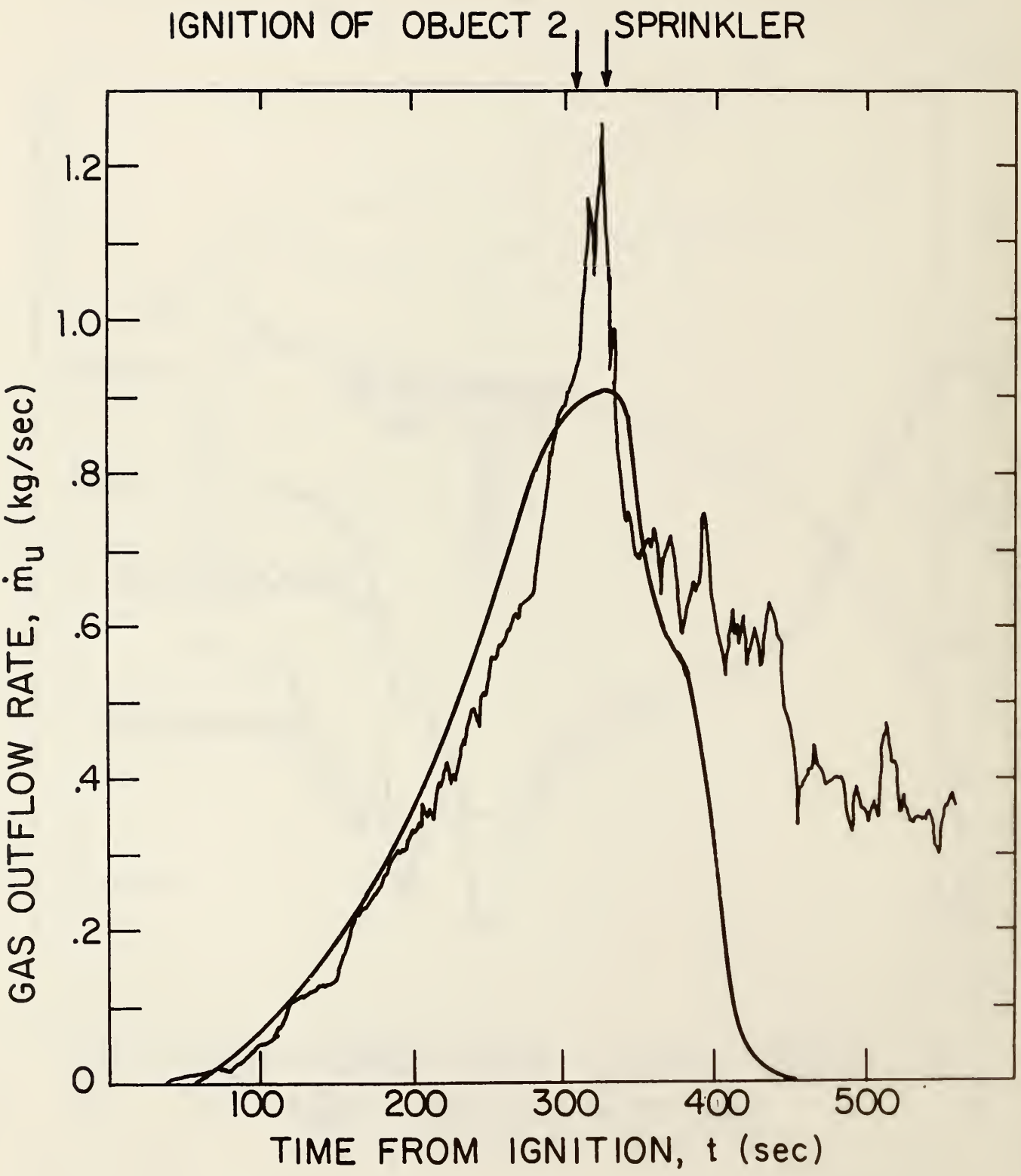
IGNITION OF OBJECT 2
SPRINKLER
1.2
1.0
.8
.6
.4
.2
0
GAS OUTFLOW RATE, $\dot{m}_u$ (kg/sec)
100
200
300
400
500
TIME FROM IGNITION, t (sec)

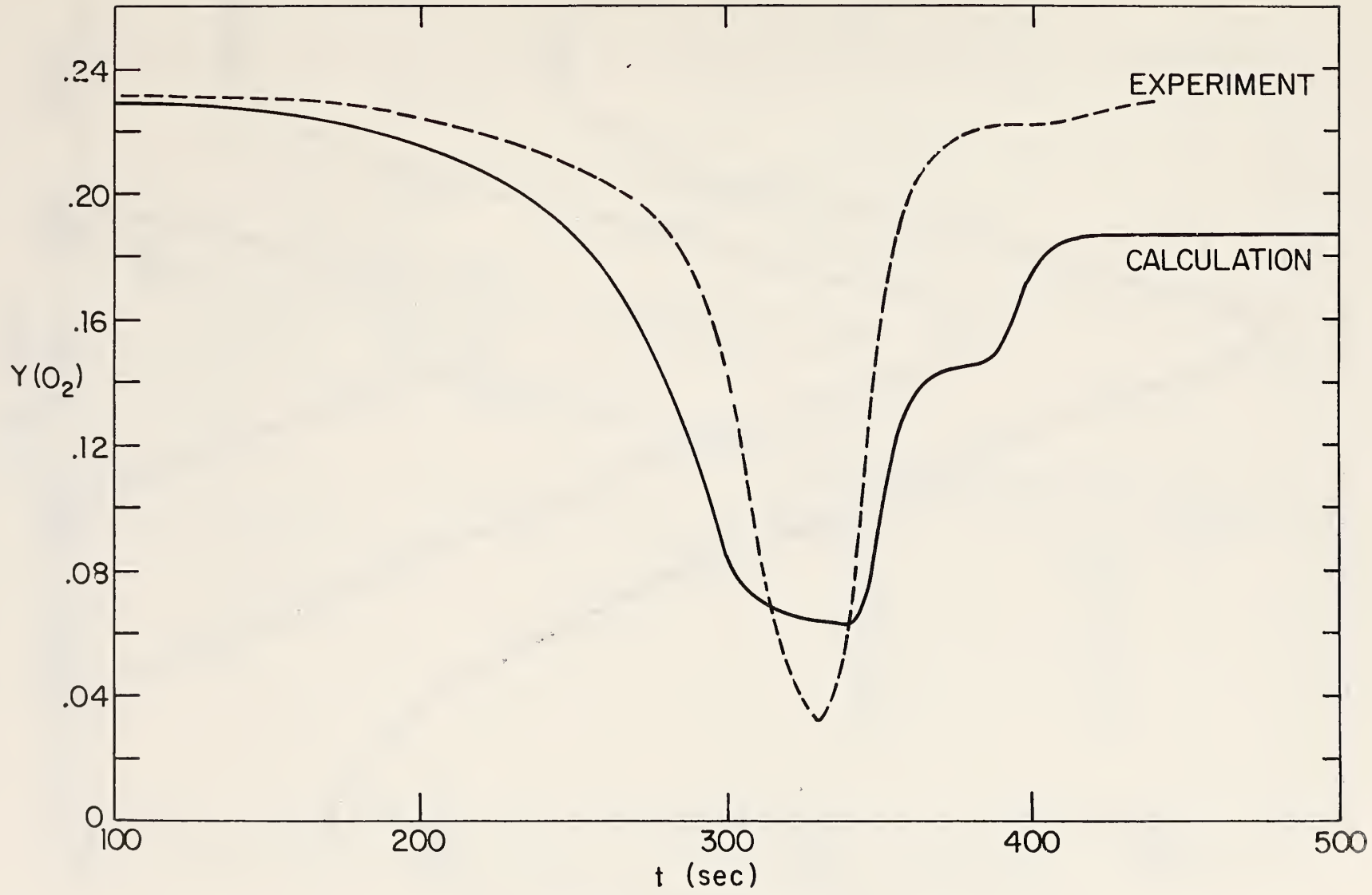
.24
.20
.16
.12
.08
.04
0
Y(O2)
100
200
300
400
500
t (sec)
EXPERIMENT
CALCULATION

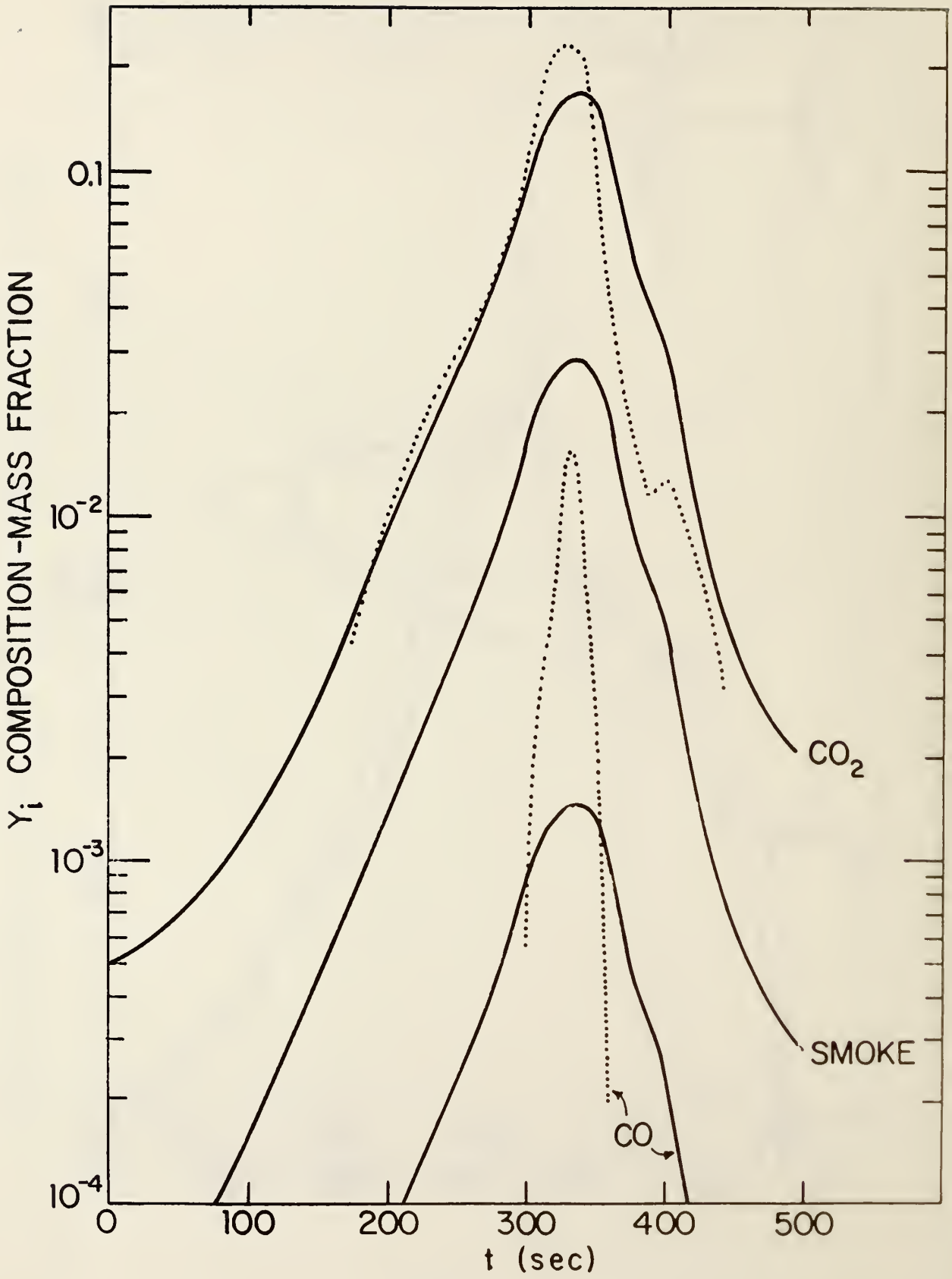
0.1
10^{-2}
10^{-3}
10^{-4}
Y_i COMPOSITION-MASS FRACTION
0
100
200
300
400
500
t (sec)
CO_2
SMOKE
CO

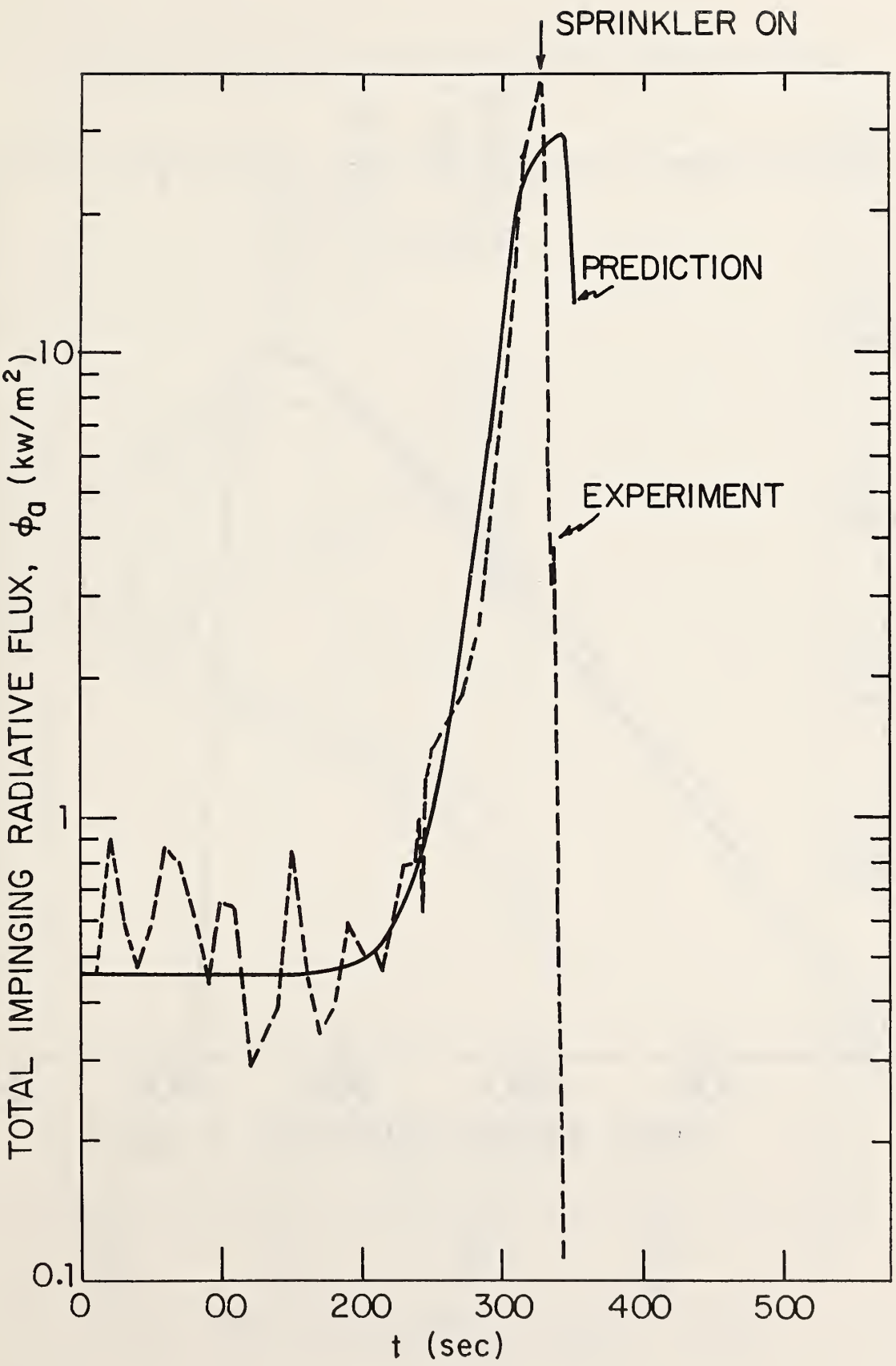
SPRINKLER ON
PREDICTION
EXPERIMENT
TOTAL IMPINGING RADIATIVE FLUX, ϕ_a (kw/m^2)
10
1
0.1
0
00
200
300
400
500
t (sec)

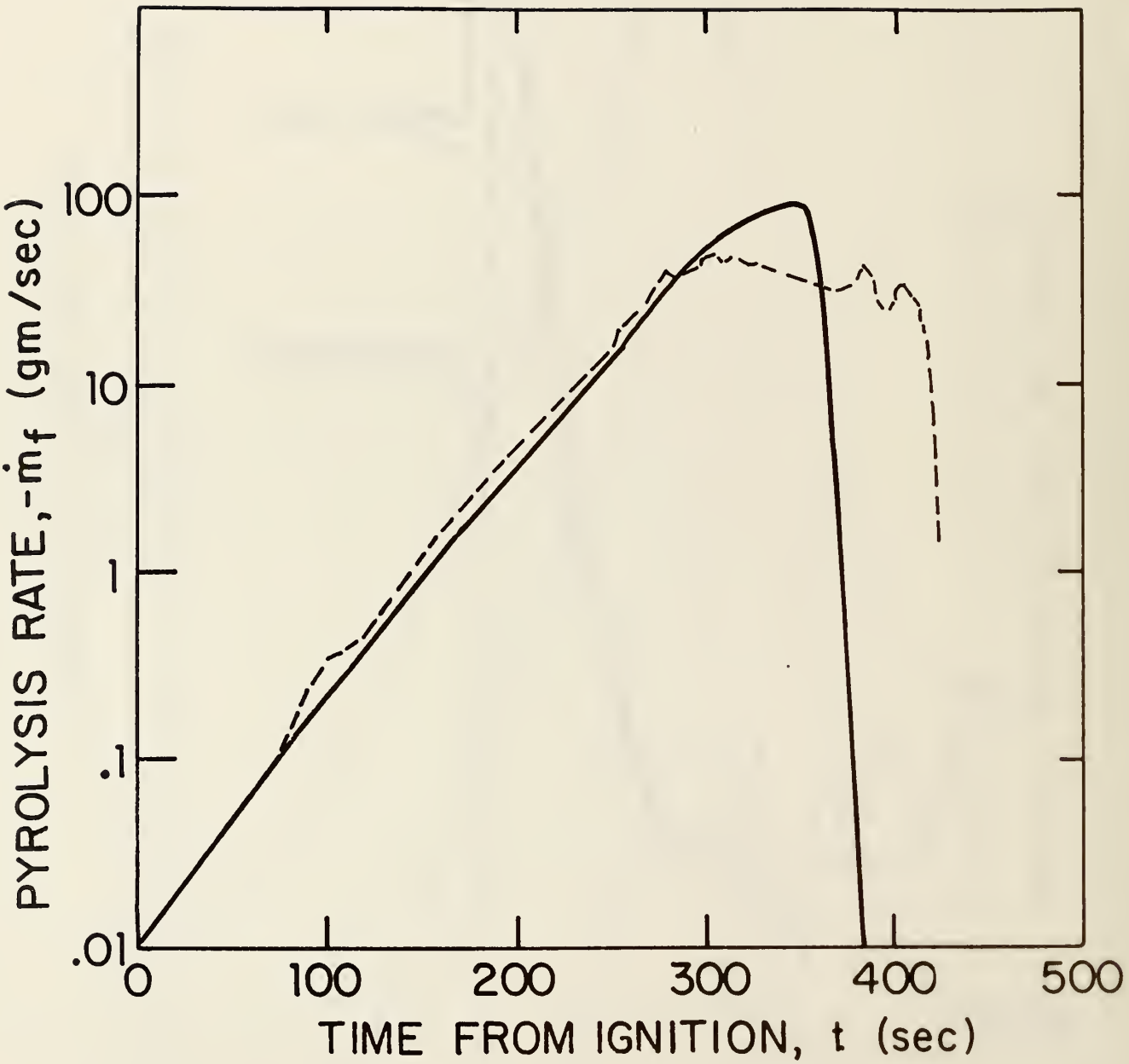
PYROLYSIS RATE, $-\dot{m}_f$ (gm/sec)
100
10
1
.1
.01
0
100
200
300
400
500
TIME FROM IGNITION, t (sec)

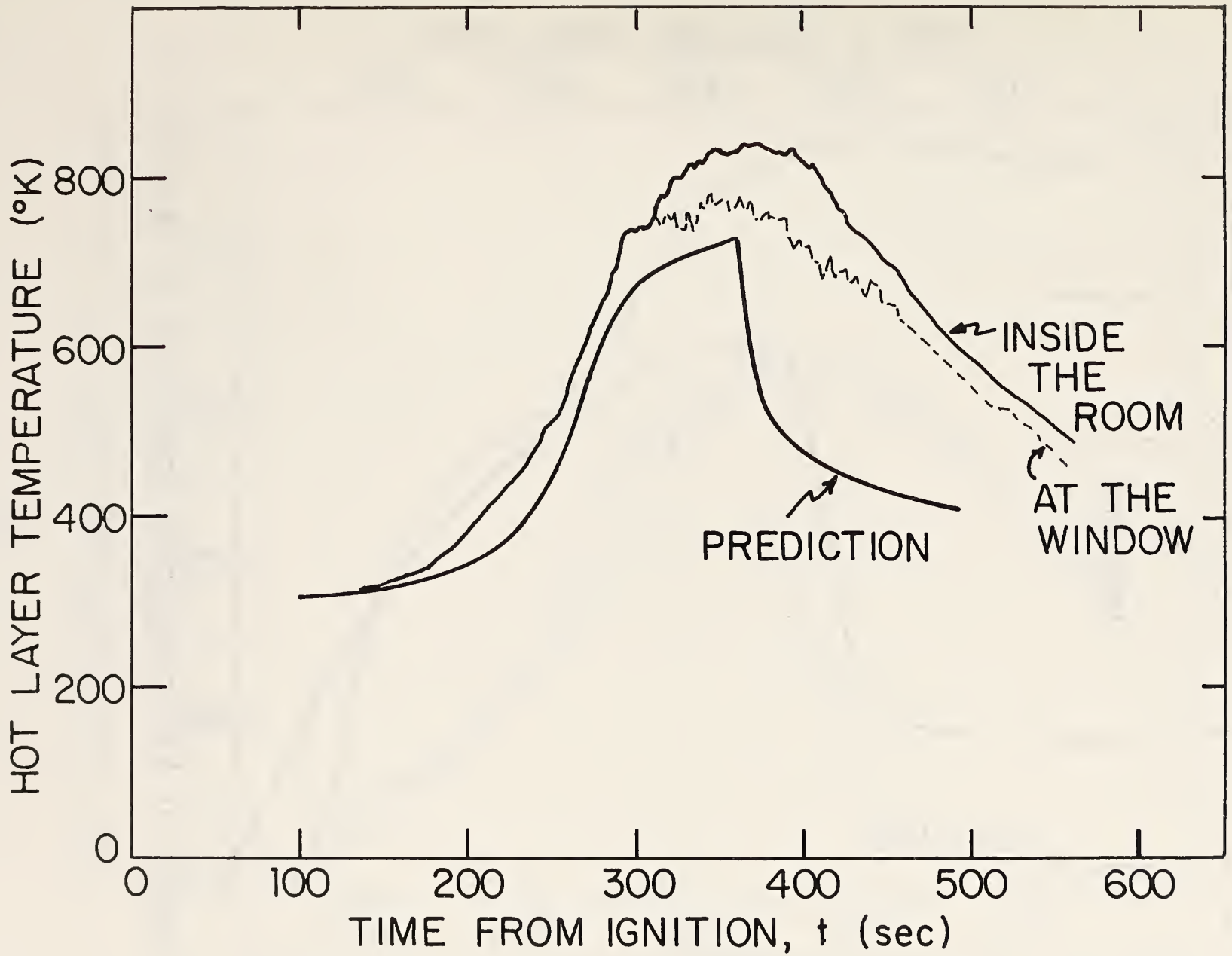
HOT LAYER TEMPERATURE (°K)
0
200
400
600
800
0
100
200
300
400
500
600
TIME FROM IGNITION, t (sec)
INSIDE THE ROOM
AT THE WINDOW
PREDICTION

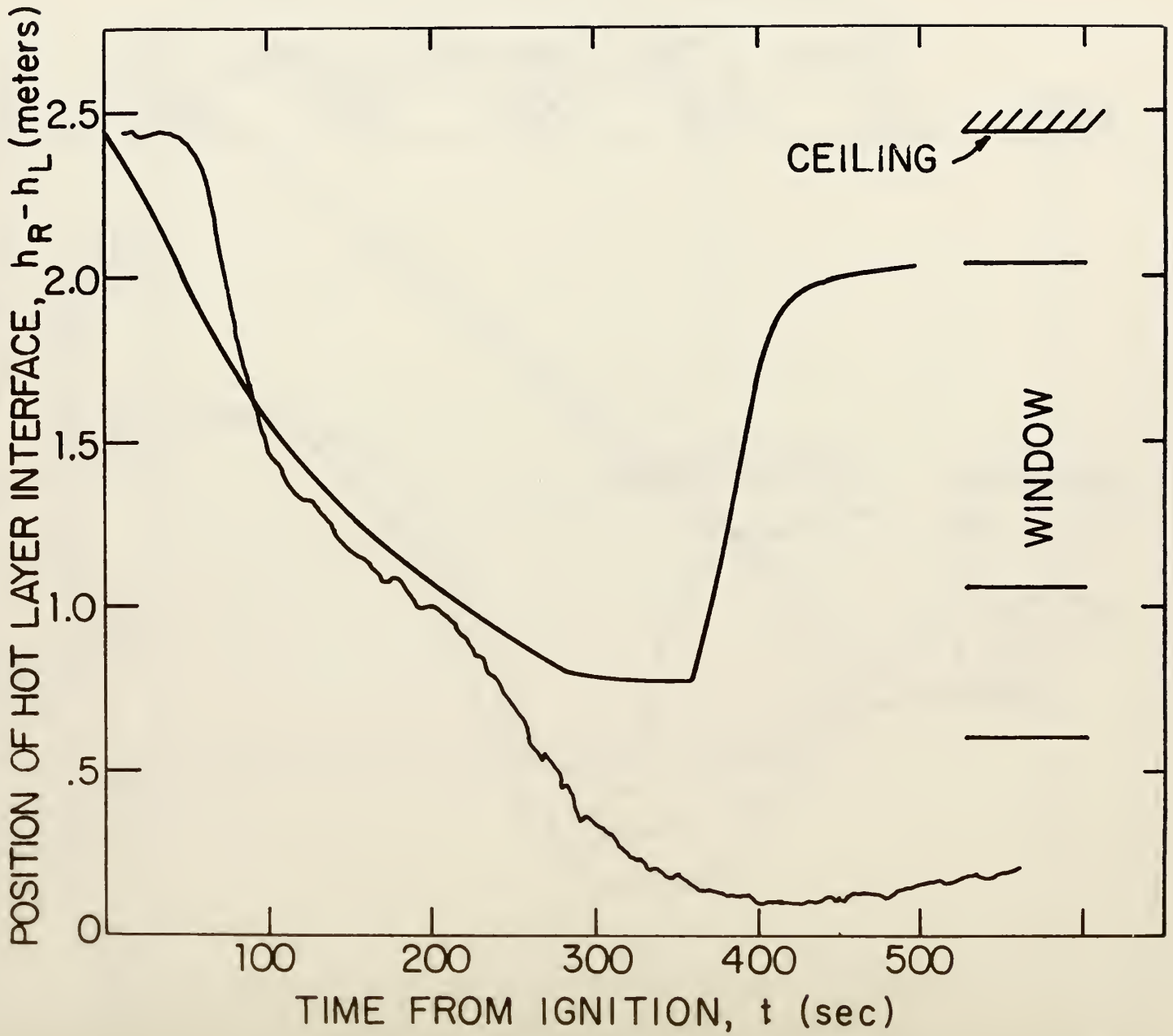
POSITION OF HOT LAYER INTERFACE, $h_R - h_L$ (meters)
2.5
2.0
1.5
1.0
.5
0
100
200
300
400
500
TIME FROM IGNITION, t (sec)
CEILING
WINDOW

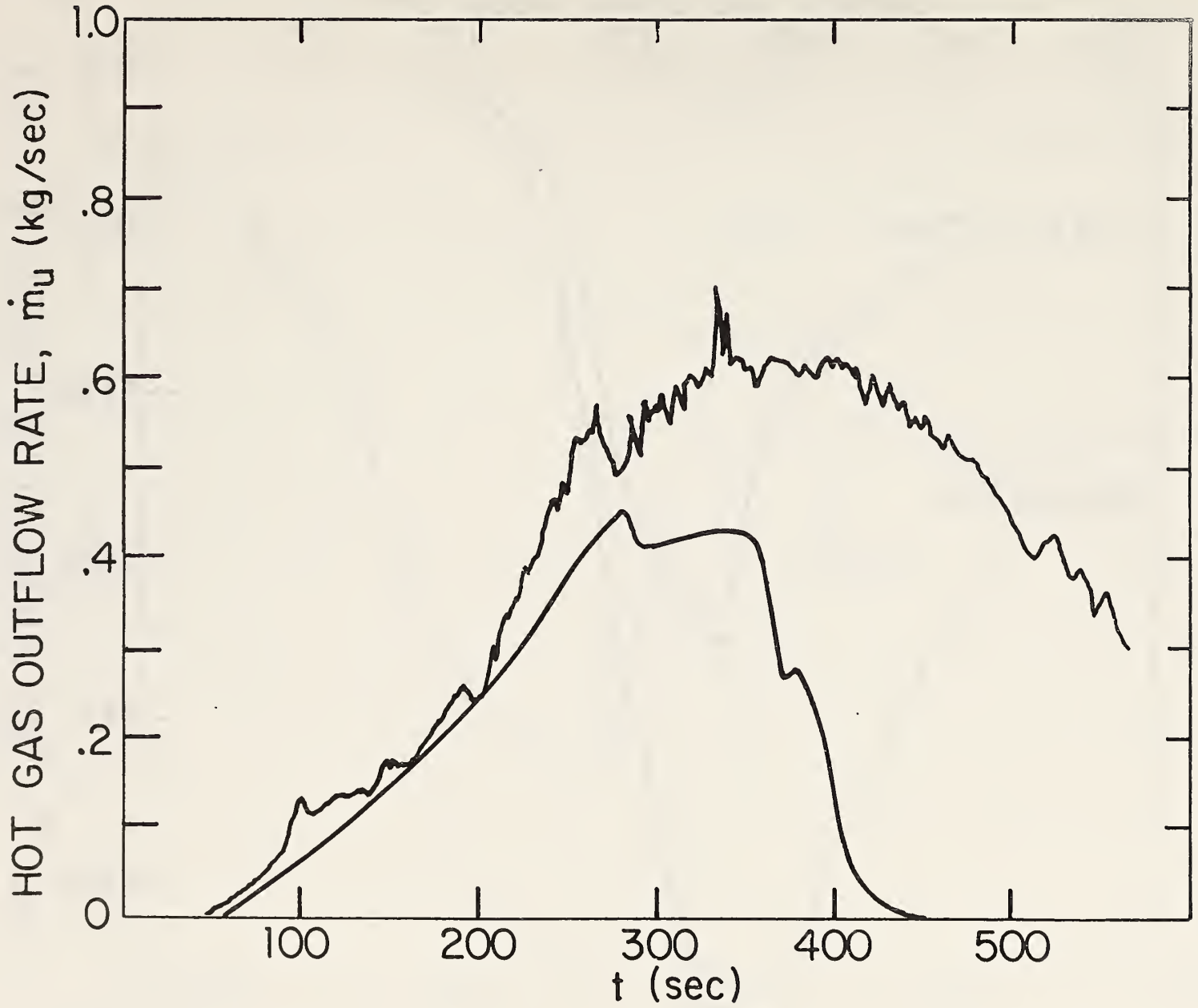
HOT GAS OUTFLOW RATE, $\dot{m}_u$ (kg/sec)
1.0
.8
.6
.4
.2
0
100
200
300
400
500
t (sec)

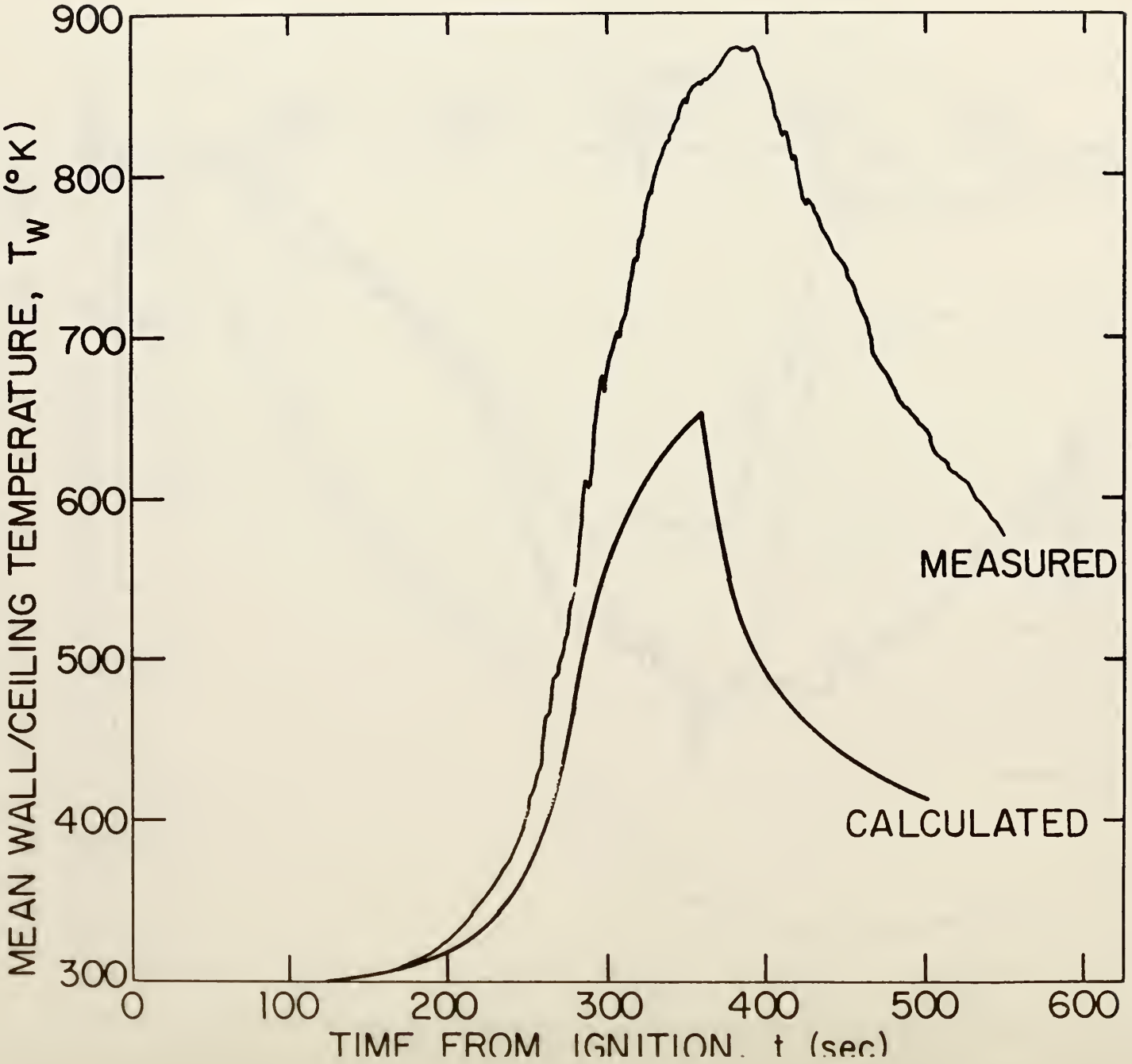
900
800
700
600
500
400
300
MEAN WALL/CEILING TEMPERATURE, T_W (°K)
0
100
200
300
400
500
600
TIME FROM IGNITION, t (sec)
MEASURED
CALCULATED

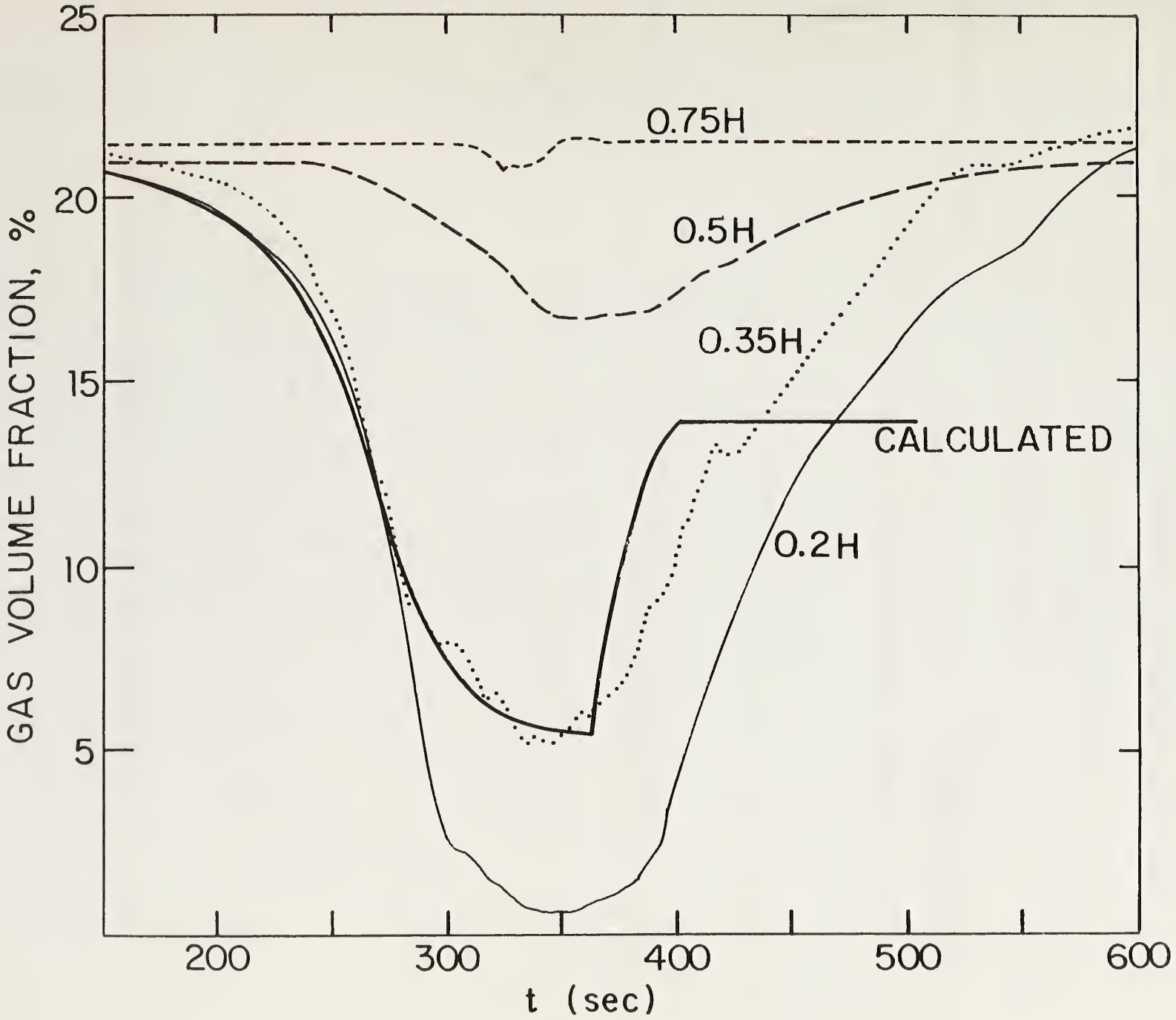
25
20
15
10
5
GAS VOLUME FRACTION, %
0.75H
0.5H
0.35H
CALCULATED
0.2H
200
300
400
500
600
t (sec)

NBS-114A (REV. 2-8C)

U.S. DEPT. OF COMM. BIBLIOGRAPHIC DATA SHEET (See instructions)	1. PUBLICATION OR REPORT NO. NBSIR-86/3459	2. Performing Organ. Report No.	3. Publication Date December 1986

4. TITLE AND SUBTITLE

How Accurate is Mathematical Fire Modeling?

5. AUTHOR(S)
Henri E. Mitler and John A. Rockett

6. PERFORMING ORGANIZATION (If joint or other than NBS, see instructions)

NATIONAL BUREAU OF STANDARDS
DEPARTMENT OF COMMERCE
~~WASHINGTON, D.C. 20234~~ Gaithersburg, Maryland 20899

7. Contract/Grant No.

8. Type of Report & Period Covered

9. SPONSORING ORGANIZATION NAME AND COMPLETE ADDRESS (Street, City, State, ZIP)

10. SUPPLEMENTARY NOTES

☐ Document describes a computer program; SF-185, FIPS Software Summary, is attached.

11. ABSTRACT (A 200-word or less factual summary of most significant information. If document includes a significant bibliography or literature survey, mention it here)

It is important to be able to predict the development of a fire in an enclosure of arbitrary complexity. A mathematical model valid for a single room, with multiple vents and objects in it has been developed. The fifth version of the model has just been completed; it is the Harvard Computer Fire Code V, or Mark 5 for short. In 1977, Factory Mutual Research Corporation carried out a series of eight well-instrumented full scale room fires, against which the single room model can be tested. The test fire room was 2.44 m x 3.66 m x 2.44 m high, with an open doorway; a slab of polyurethane foam in one corner, and a polyurethane foam target in a facing corner. The primary slab was ignited at its center, and the fire followed. The other tests were variants of this one. We compare the results of the calculations with the results of two of the experiments: the standard configuration and the case with a window replacing the doorway. The model "predictions" are in good to excellent agreement for most of the variables. The disagreements are discussed, and it is found that the most probable causes of disagreements are failure to take heating of the lower gas layer into account, inadequacy of the burnout algorithm, and lack of understanding of the production mechanism of CO.

12. KEY WORDS (Six to twelve entries; alphabetical order; capitalize only proper names; and separate key words by semicolons)
compartment fires; computer programs; fire models; mathematical models; room fires

13. AVAILABILITY

☒ Unlimited

☐ For Official Distribution. Do Not Release to NTIS

☐ Order From Superintendent of Documents, U.S. Government Printing Office, Washington, D.C. 20402.

☒ Order From National Technical Information Service (NTIS), Springfield, VA. 22161

14. NO. OF PRINTED PAGES
50

15. Price
$9.95

USCOMM-DC 6043-P80